虫による脳肺吸虫症の報告では30歳以下が圧倒的に多く，特に10歳以下の小児が40-60％を占めていた[1]．メキシコ肺吸虫の報告でも5-8歳(3症例)の小児であり[2]，最近の中国における報告でも脳肺吸虫症は若年層男性に多い[3]．

2）住血吸虫症

人体に寄生する住血吸虫のうち神経症状が報告されているのは，ビルハルツ住血吸虫(*Schistosoma haematobium*)，マンソン住血吸虫(*S. mansoni*)，日本住血吸虫(*S. japonicum*)，メコン住血吸虫(*S. mekongi*)の4種類で，前2種では主に脊髄病変，後2種では主に大脳皮質の病変が報告されている．それぞれの種の分布域は，ビルハルツ住血吸虫がアフリカと中近東，マンソン住血吸虫がアフリカと中近東および中南米の一部，日本住血吸虫が中国の揚子江流域とフィリピンなどの東アジア，メコン住血吸虫はメコン川流域の東南アジアである．

住血吸虫類は，吸虫の中では例外的に第2中間宿主を必要とせず，第1中間宿主の貝から水中に遊出した感染型の幼虫(セルカリア)が，直接終宿主に経皮感染する．したがって住血吸虫症は食品由来ではなく，中間宿主貝が生息する河川や湖沼での農作業や漁撈，遊泳など，水との接触に伴って感染する．

3. 病　　態

1）肺吸虫症

病態の基本は，虫体そのものと虫体周囲の好酸球性炎症による組織破壊である．炎症の部位によって髄膜刺激症状や出血も起こしうる．食品とともに経口摂取されたメタセルカリアは消化管から腹腔内へ出て，腹壁の結合組織や筋肉内に入り込んでおよそ2週間ほどして再度腹腔に戻り，そこから次に肝臓/横隔膜を通過して胸腔に入る．そして肺の胸膜を破って肺実質へ侵入する．

このような体内移行経路をとるため，途中で様々な部位に侵入しうる．中枢神経系への侵入経路は必ずしも確定していないが，体内移行の途中に腹腔から血行性に脊髄腔へ入り頭蓋内に入る経路，縦隔の軟部組織を上行して頸静脈に沿って頭蓋腔へ入る経路，および頸静脈内を上行して横洞内を経て脳実質へ入るという経路が推測されている[4]．

2）住血吸虫症

住血吸虫のセルカリアは，経皮感染後に血流に乗って肺に至り，血管内を移動して成虫になる．寄生部位は，ビルハルツ住血吸虫は膀胱近傍の静脈系，マンソン住血吸虫や日本住血吸虫は，腸間膜静脈-肝門脈系である．

神経型住血吸虫症は感染者全体の2-4％で報告されるが，比較的報告数が多い日本住血吸虫症では大脳皮質の病変が中心で，ビルハルツ住血吸虫，マンソン住血吸虫症では，より下位の脊髄病変が多い．神経型住血吸虫症は，虫卵による病変が直接の病因となっている直接型と，肝性脳症による間接型に分けて考えると理解しやすい．

a. 直 接 型

住血吸虫卵による中枢神経系血管内の塞栓で生じるもの，虫卵塞栓を核にした肉芽腫によるもの，肉芽腫血管炎や虫体・虫卵の代謝産物による炎症性変化で生じるものなどに分けて考えることができる．前者では，脳血管障害でみられるような巣症状が中心となるが，後者では，髄膜炎・脳炎様症状が伴うことがある[5,6]．

大量の住血吸虫セルカリアに同時に感染した場合，片山症候群といわれる急激な発熱に続き，咳や腹部膨満感，頭痛・嘔吐・痙攣・意識障害といった急性髄膜脳炎の症状を示すことがある．非特異的な急性症状が中心で，好酸球増多を示す例が多くステロイド治療に反応することから，虫卵塞栓よりも免疫反応活性化の関与が大きいと思われる．

慢性期には，神経系の他の虚血性病変でもみられる多彩な巣症状と，病変の中心が皮質にある場合は，痙攣発作で始まることが多い．発作型は，大発作は20％程度で部分発作が残りの大半を占める[7]．初発作後に上肢の単麻痺や片麻痺，失語症や視野障害などを合併することが多く，局在性病巣による巣症状は，一過性のこともあれば継続する場合もある．発作の頻度は，病初期には多いが次第に減少していく．中枢神

経系血管内の虫卵塞栓と肉芽腫性変化が病変の主体なので，一定期間住血吸虫有病地に居住し，感染を繰り返した感染期間が長い例での発症がほとんどである．

b. 間 接 型

門脈圧亢進症が進行した結果，側副血行路が形成され，門脈系と体循環系の静脈間にシャントが生じることで高アンモニア血症による肝性脳症を示すことがある．また，住血吸虫症性肝硬変も肝性脳症の要因となる[7,8]．しかし，住血吸虫症では門脈域中心の肝線維化が明らかな段階でも肝実質・類洞の障害は軽微なので，肝機能低下が肝性脳症に及ぼす影響は，ウイルス肝炎での肝硬変とは異なり小さい．

4. 診断と鑑別診断

1) 肺吸虫症

肺吸虫の中枢神経系への迷入では，その時期，迷入部位，虫体数など様々な要因が絡むために症状は多様であり，肺吸虫感染に固有の症状はない．脳肺吸虫症の画像上の一般的な特徴は，浮腫を伴うリング影の集合体(ブドウの房様あるいは石けん泡様と表現される)とされるが，必ずしも典型的な画像所見を呈するものではなく，出血が最も多かったとする報告もある[9,10]．

肺吸虫症では，虫卵が喀痰や胸水中，あるいは気管支肺胞洗浄液中に見いだされることがあるので，これが検出できれば確定診断となる．糞便からの検出率は高くないが試みる価値は十分にある．虫卵の検出と同時に施行すべきなのは，血清ならびに髄液や胸水など局所液の抗体検査である．抗体検査はあくまで補助診断法であるとはいえ，特に肺吸虫症においては非常に有効である．国内の肺吸虫症例の多くは少数の虫体寄生による軽症例のため虫卵検出率は低く，抗体検査で診断され治療されている症例がほとんどである．

酵素抗体法(ELISA)を用いた寄生虫疾患抗体スクリーニング検査は(株)エスアールエルで実施されている．対象項目にウエステルマン肺吸虫と宮崎肺吸虫が含まれるので，肺吸虫症の診断には大いに役に立つ．宮崎大学医学部・感染症学講座・寄生虫学分野でも同様の検査を実施しており，エスアールエルがカバーしていない住血吸虫症や広東住血線虫症にも対応している．

2) 住血吸虫症

住血吸虫症の確定診断は虫卵検査での陽性だが，最近は，腹部超音波検査などで見つかるケースも増えている．神経型でも，CTやMRIによる画像検査での鑑別診断が重要である．治療の適否を決定するためには，虫卵検査が陰性であった場合も，ELISAなどの抗体検査，必要に応じてPCRなども利用した確定診断を行う必要がある．

a. 直 接 型

a) 急性神経型住血吸虫症

急性髄膜脳炎の症状を示すが，髄液検査では，圧がやや高く単球優位のわずかな細胞増加を認める以外，所見に乏しいことが多い[7]．末梢血検査で好酸球増多を示し，糞便や尿中に虫卵を認めれば確定診断に至る．感染初期は，抗体検査が陽性にならないこともある．頭部CTやMRIでは，軽度の脳圧亢進を示すびまん性の腫大が認められることがある．

b) 慢性神経型住血吸虫症

神経系の巣症状を示す脳腫瘍や脳血管障害，痙攣発作を示すてんかんとの鑑別が重要となる．住血吸虫卵の検出は難しいことが多く，好酸球増多などの所見もみられないが，抗体検査は陽性である．神経系の病巣はCTでは単発，多発する低吸収巣として認められ，炎症性変化が強い肉芽腫性病変は周辺の増強効果をみることもある[11,12]．MRIでは，T1強調画像では低信号，T2強調画像では高信号となるのが一般的だが，脳腫瘍や他の炎症性変化に比べると比較的均一な病変となる[12]．脳波検査では，汎性α波パターンに散在性，突発性の徐波の混入をみる[7,8]．

b. 間 接 型

再感染を繰り返す例を除き，住血吸虫卵が検出されることはなく，経過が長い場合には抗体検査も陰性となることがある．日本住血吸虫感染の後遺症とでもいうべき時期で，日本住血感染の既往歴と高アンモニア血症，脳波検査での三相波から，ほかの代謝性脳症と鑑別診断さ

れる[8]．

5. 治療と予後

肝蛭を除いたすべての吸虫感染症はプラジカンテル(商品名：ビルトリシド，バイエル)が著効を示す．ただし，肺吸虫症と住血吸虫症の両者ともに国内では適応外薬である．プラジカンテルは副作用は少ないが，時に発熱，腹部不快感，悪心，下痢，頭痛などがみられる．妊婦への安全性は確立されていないため，妊娠4カ月未満の妊婦への投与は避ける．

1) 肺吸虫症

プラジカンテルを75mg/kg/日，分3で3日間内服する．添付文書では40mg/kg/日，分2，2日間投与と指示されているが，これまでの経験から75mg/kg/日が推奨されている[13]．大量胸水貯留例では，投薬前に胸水をできるかぎり除去しておくことが望ましい．服薬後に，急性期であれば虫体の死滅によって多量の抗原が放出され，一過性に末梢好酸球値が上昇することがある．好酸球値は次第に正常化し，これと並行して画像所見が改善し，時間をかけて特異抗体が消失していく．予後は良好である．

2) 住血吸虫症

神経型の治療でもプラジカンテルが基本で，急性型ではコルチコステロイドも併用される．抗けいれん剤が必要な場合も，プラジカンテル投与後しばらくすると併用の必要がなくなることが多い．虫卵が石灰化し，痙攣発作の焦点となってしまった場合には外科的な処置が必要になることがある[14]．

プラジカンテルは，集団投与では，40mg/kgでの1回投与が国際的に汎用されるが，この標準的治療を何回か受けていた中国の日本住血吸虫症例で，神経症状が難治となり外科的手術が必要になった報告がある[14]．プラジカンテルの用量については，50-60mg/kg/日，分2の経口投与で，神経症状の良好な予後が得られている[15]．糞便中に虫卵が確認されなくても，虫卵抗原に対する抗体価が高い場合もプラジカンテル投与の適応はある．

おわりに

寄生虫疾患は全体の頻度も高くないので，例外的な場合を除いて，神経症状を呈する症例で真っ先に寄生虫感染を疑うということはない．しかしながら，髄液中に好酸球が多数出現していたり，あるいは感染症を疑わせるにもかかわらず細菌性やウイルス性らしくないときには，寄生虫という可能性も考慮すべきである．そのときには，抗体検査などで積極的に検索することが診断と治療に直結する．

(本稿は，厚生労働科学研究費補助金　医療技術実用化総合研究事業‘わが国における熱帯病・寄生虫症の最適な診断治療体制の構築’(H25-医療技術-指定-012)の成果を含む)

文献

1) Higashi K, et al: Cerebral paragonimiasis. J Neurosurg 34: 515-527, 1971.
2) Brenes Madrigal R, et al: Cerebral hemorrhagic lesions produced by *Paragonimus mexicanus*. Report of three cases in Costa Rica. Am J Trop Med Hyg 31(3 Pt 1): 522-526, 1982.
3) Zhang JS, et al: MRI features of pediatric cerebral paragonimiasis in the active stage. J Magn Reson Imaging 23: 569-573, 2006.
4) Katchanov J, Nawa Y: Helminthic invasion of the central nervous system: many roads lead to Rome. Parasitol Int 59: 491-496, 2010.
5) Ferrari TC, Moreira PR: Neuroschistosomiasis: clinical symptoms and pathogenesis. Lancet Neurol 10: 853-864, 2011.
6) Ross AG, et al: Neuroschistosomiasis. J Neurol 259: 22-32, 2012.
7) 林　正高：急性及び慢性日本住血吸虫症と脳機能障害との関係．地方病とのたたかい，p208-247，山梨地方病撲滅協会，1981.
8) Hayashi M: Clinical features of cerebral schistosomiasis, especially in cerebral and hepa-

tosplenic type. Parasitol Int 52: 375-383, 2003.
9) Cha SH, et al: Cerebral paragonimiasis in early active stage: CT and MR features. AJR Am J Roentgenol 162: 141-145, 1994.
10) Chen J, et al: Cerebral paragonimiasis that manifested as intracranial hemorrhage. J Neurosurg Pediatr 6: 572-578, 2010.
11) Ohmae H, et al: Imaging diagnosis of schistosomiasis japonica—The use in Japan and application for the field study in the present endemic area—. Parasitol Int 52: 385-393, 2003.
12) Preidler KW, et al: Cerebral schistosomiasis: MR and CT appearance. AJNR Am J Neuroradiol 17: 1598-1600, 1996.
13) 熱帯病治療薬研究班：寄生虫症薬物治療の手引き2010(以下のURLからダウンロード可[http://www.med.miyazaki-u.ac.jp/parasitology/orphan/HTML/page-DL.htm]).
14) Ting L, et al: Surgical treatment of epilepsy with chronic cerebral granuloma caused by *Schistosoma japonicum*. Epilepsia 49: 73-79, 2008.
15) Watt G, et al: Praziquantel in treatment of cerebral schistosomiasis. Lancet 8506: 529-532, 1986.

J. Biochem. 2013;153(3):267–273 doi:10.1093/jb/mvs135

JB THE JOURNAL OF BIOCHEMISTRY

Pharmacophore identification of ascofuranone, potent inhibitor of cyanide-insensitive alternative oxidase of *Trypanosoma brucei*

Received October 15, 2012; accepted November 6, 2012; published online November 23, 2012

Hiroyuki Saimoto[1], Yasutoshi Kido[2,*], Yasushi Haga[1], Kimitoshi Sakamoto[2,†] and Kiyoshi Kita[2,‡]

[1]Department of Chemistry and Biotechnology, Graduate School of Engineering, Tottori University, Tottori 680-8552, Japan; and [2]Department f Biomedical Chemistry, Graduate School of Medicine, The University of Tokyo, Tokyo 113-0033, Japan

*Yasutoshi Kido, Department of Biomedical Chemistry, Graduate School of Medicine, University of Tokyo, 7-3-1 Hongo, Bunkyo-ku, Tokyo 113-0033, Japan. Tel: +81-3-5841-3526, Fax: +81-3-5841-3444, email: yasutoshikido@gmail.com

‡Kiyoshi Kita, Department of Biomedical Chemistry, Graduate School of Medicine, University of Tokyo, 7-3-1 Hongo, Bunkyo-ku, Tokyo 113-0033, Japan. Tel: +81-3-5841-3526; Fax: +81-3-5841-3444; email: kitak@m.u-tokyo.ac.jp

†Present address: Kimitoshi Sakamoto, Faculty of Agriculture and Life Science, Hirosaki University, Hirosaki 036-8561, Japan.

***Trypanosoma brucei* is a parasite that causes human African trypanosomiasis (HAT). The parasites depend on the cyanide-insensitive trypanosome alternative oxidase (TAO) for their vital aerobic respiration. Ascofuranone (AF), a potent and specific sub-nanomolar inhibitor of the TAO quinol oxidase, is a potential novel drug with selectivity for HAT, because mammalian hosts lack the enzyme. To elucidate not only the inhibition mechanism but also the inhibitor–enzyme interaction, AF derivatives were designed and synthesized, and the structure–activity relationship was evaluated. Here we identified the pharmacophore of AF that interacts with TAO. The detailed inhibitory profiles indicated that the 1-formyl and 6-hydroxyl groups, which might contribute to intramolecular hydrogen bonding and/or serve as hydrogen-bonding donors, were responsible for direct interaction with the enzyme.**

Keywords: alternative oxidase/ascofuranone/neglected tropical disease/trypanosome/structure–activity relationship.

Abbreviations: AF, ascofuranone; AOX, alternative oxidase; HAT, human African trypanosomiasis; IC_{50}, 50% inhibitory concentration; rAOX, recombinant alternative oxidase; rTAO, recombinant trypanosome alternative oxidase; SAR, structure–activity relationship; SHAM, salicyl hydroxamic acid; TAO, trypanosome alternative oxidase.

Trypanosoma brucei, which causes human African trypanosomiasis (HAT), depends on a cyanide-insensitive respiratory pathway for survival (*1*). Such cyanide-insensitive oxygen consumption has been recognized in plants since 1920s (*2*). Intensive biochemical studies revealed that a mitochondrial membrane enzyme, designated alternative oxidase (AOX), is responsible for cyanide-insensitive respiration (*1–3*). To date, AOX has been detected not only in higher plants and protozoa including trypanosomes but also in algae, yeast, slime moulds, free-living amoebae, eubacteria and nematodes (*4*, *5*).

The cyanide-insensitive ubiquinol oxidase activity of AOX catalyzes the four-electron reduction of dioxygen to water and has been characterized as a salicyl hydroxamic acid (SHAM)-inhibited activity (*6*). Although the activity inhibited by SHAM has been assigned to the ubiquinol oxidase moiety of AOX, inhibition of the activity requires a relatively high concentration (micromolar) of SHAM (*6*, *7*). We previously reported that ascofuranone (AF), isolated from pathogenic fungus *Ascochyta viciae*, specifically inhibits the ubiquinol oxidase activity of trypanosome mitochondrial AOX (TAO) at sub-nanomolar levels, revealing a novel class of potent AOX inhibitors (*8*). Furthermore, since TAO is essential for trypanosomal survival and is absent from mammalian hosts, AF represents a lead compound for development of selective anti-HAT drugs (*1*, *9*, *10*). Indeed, we have demonstrated the chemotherapeutic efficacy of AF both *in vitro* and *in vivo* (*8*, *11*, *12*). However, the structural requirements for AF inhibition of AOX remain poorly defined.

In this study we have designed and synthesized derivatives of AF. Biochemical evaluation of the derivatives elucidates the relationship between the chemical structures and inhibition of TAO. The structure–activity relationship (SAR) study for the inhibition of TAO identified the profile of the AF pharmacophore. Our data shed light upon the potential for drug development for HAT, a neglected tropical disease, while also clarifying the molecular interaction between AF and TAO.

Materials and Methods

Production of recombinant TAO and recombinant Sauromatum gutattum AOX

Recombinant TAO (rTAO) was produced using a haeme synthesis-deficient strain (FN102) harbouring a TAO-encoding plasmid, as described in a previous study (*13*). The strain FN102/pTbAO was grown aerobically at 30°C and induced to express rTAO. Inner membranes from the induced strain were used to assay enzymatic activity in the presence of a series of AF derivatives. The 50% inhibitory concentration (IC_{50}), which is a molar concentration needed to halve the control enzymatic activity, was used to evaluate the inhibitory activity. Recombinant *S. gutattum* AOX was also produced using FN102 harbouring a *S. gutattum* AOX-encoding plasmid as rTAO was expressed.

Ubiquinol oxidase assay

Ubiquinol oxidase activity was measured by recording the absorbance change of ubiquinol-1 ($\varepsilon_{278} = 15{,}000\,M^{-1}cm^{-1}$) at 278 nm (SHIMADZU spectrophotometer UV-3000). Reactions (1 ml each) were constituted from 0.35 μg of FN102/pTbAO membrane fraction in 50 mM Tris–HCl (pH 7.3). Following pre-incubation (2 min at 25°C), reactions were initiated by the addition of ubiquinol-1 to a final concentration of 150 μM. The sigmoidal curve of the inhibition was observed using a broad dilution series of all AF derivatives ranged from none of inhibition to complete inhibition. Following the depiction of the sigmoidal curve, a sequential analysis of the inhibition was performed using at least five different concentrations of all AF derivatives around IC_{50} values. The measurement of ubiquinol oxidase activity of recombinant *S. gutattum* AOX was identical to that of rTAO. The presence of dithiothreitol in the ubiquinol oxidase assay of rTAO does not affect the activity at all despite other AOX's activity occasionally regulated by a disulphide/sulphhydryl system via conserved cysteine residue.

Synthesis of test compounds

A series of AF derivatives synthesized and tested in this study are numbered from 1 to 30. The synthetic procedures are described in the Supplementary data.

Results and Discussions

The chemical structure of AF (Fig. 1A) consists of three moieties: aromatic ring, linker and furanone ring. The functional groups at those moieties were chemically modified and synthesized. The inhibitory activity of all AF derivatives was evaluated for ubiquinol oxidase activity of rTAO by IC_{50}. At nanomolar concentrations, AF inhibits not only rTAO but also recombinant AOXs (rAOXs) derived from other organisms such as plants and pathogenic microorganisms, although AOXs have diverse and unique physiological functions in each organism (*14*, *15*). Table I summarizes the IC_{50}s for rAOXs from various organisms, suggesting that AF is a potent and universal inhibitor of various AOXs (*13*, *15*).

For rTAO tested under our experimental conditions, the IC_{50} of AF was 0.13 nM. For comparison, the IC_{50}s of SHAM and ascochlorin (Fig. 1B; another metabolite from the fungus *A. viciae*) were 4 μM and 1.5 nM, respectively. This difference between AF and ascochlorin suggested that the structure and asymmetric carbon at the furanone ring might be involved in the binding to TAO as judged from the structural relation between the two compounds. However, a significant difference was not observed in the derivatives in which the furanone ring was substituted, as demonstrated by the IC_{50}s for colletochlorin B (0.20 nM) and compound **1** (0.40 nM) (Table II). The other furanone ring-substituted derivatives (**2** and **3**) showed potencies (1.2 and 1.4 nM, respectively) similar to that of ascochlorin. These data indicated that the furanone ring was not essential for the strong inhibition of AF. The linker structure might interact with the enzyme because the linker of ascochlorin was different from the geranyl chain of AF.

To confirm the function of the geranyl chain, we synthesized and investigated a series of compounds that replaced the linear alkyl chain while maintaining the furanone ring as in AF (as shown in Table III). The IC_{50}s of compounds **4** (with two branched methyl groups), **5** (with a Cα-double bond) and **6** (with a linear alkyl chain) were 0.30, 1.0 and 0.5 nM, respectively. Thus, the IC_{50} of each of these derivatives was several times as high as that of AF. Although the geranyl structure of AF was obviously favourable for inhibition, the linker structure was likely to be flexible to inhibit TAO strongly at a nanomolar level. This slight decrease of the inhibitory activity suggested that the linker structure in the proximity of the aromatic ring may affect the conformational range available to these compounds.

In addition to the structure, we examined the effect of the total linker length in the inhibitory potency, as shown in Table IV. Six compounds were prepared varying the side chain length at the 5-position from propenyl (C_3) to dodec-1-enyl (C_{12}) (**7a–7f**). Table IV shows that the optimum length for potent inhibition was observed at (**7d**; C_9) and (**7e**; C_{10}). The compound with the shortest linker (**7a**; C_3) exhibited a remarkable decrease in potency (IC_{50} 1,000 times higher than that of AF), suggesting that hydrophobicity is required for inhibition, consistent with the fact that TAO is a membrane protein. In contrast, the IC_{50} values of compound (**7f**; C_{12}) with a longer chain above the optimum length seemed to be lower; we hypothesize that this compound might be trapped in the hydrophobic lipid bilayer of the membrane. A similar tendency is generally observed for other hydrophobic inhibitors (*16*).

Since the geranyl linker and the furanone ring were not essential for potent inhibition, the effect of the steric tolerance for this portion was examined (**8**, **9** and **10**) to elucidate the interaction between AF and TAO (Table V). The size of this portion did not affect the inhibitory activity, suggesting that the chemical moiety that is attached to the C9 (or beyond) is not associated with the enzyme. In other words, those chemical structures might be located at the surface or outside of TAO in the AF–TAO complex. Such expected steric interaction between AF and TAO was supported by the fact that the inhibitory activity of **13** was much more potent than that of **11**, despite the presence of a hydroxyl group at the end of the

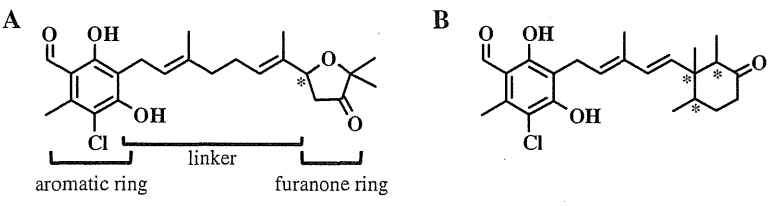

Fig. 1 Chemical structure of inhibitors of AOX. (**A**) Ascofuranone. (**B**) Ascochlorin. Asterisk represents asymmetric carbon.

Table I. IC_{50} values of ascofuranone for ubiquinol oxidase activity derived from various organisms.

Species	IC_{50} (nM)
T. brucei[a]	0.13 ± 0.04
S. gutattum[b]	1.4 ± 0.3
Antonospora locustae[c]	>91% inhibition at 10 nM
Trachipleistophora hominis[c]	>93% inhibition at 10 nM

An index 50% inhibitory concentration (IC_{50}), which is a molar concentration needed to halve the control enzymatic activity, was used to evaluate the inhibitory activity of AF for the ubiquinol oxidase activity of rAOXs from various organisms. [a]From Kido *et al.* (*13*). [b]From this study. [c]From Williams *et al.* (*15*).

Table II. TAO inhibition by furanone ring substituted derivatives.

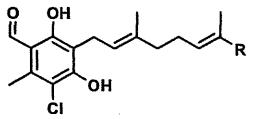

Compound	R	IC_{50} (nM)
Ascofuranone	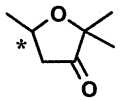	0.13 ± 0.04
Colletochlorin B	—CH_3	0.20
1	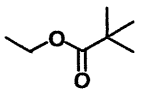	0.40
2	—OH	1.2
3	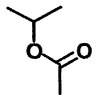	1.4

linker, which had a detrimental effect on the potency (**6** versus **12**).

Since we have recently reported that AF showed mixed-type inhibition for the TAO against ubiquinol (*13*), we speculated that the aromatic ring and the geranyl moiety of AF would be responsible for the direct interaction with TAO. To investigate the role of functional groups on the aromatic ring, AF derivatives substituted at 1-, 2-, 3- and 4-positions were synthesized and examined. The functional group at the 1-position in AF is a formyl group, and an intramolecular hydrogen bond between the 1- and 6-positions of the aromatic ring (=**O** of formyl group and —**OH** of 6-position) was expected in AF. Table VI shows the inhibitory effect of 1-position substitutions of AF on TAO. The acetyl-substituted derivatives (all containing the geranyl linker) (**14**, **15** and **16**) showed an inhibitory activity similar to that of AF, whereas the inhibitory activity was significantly decreased in the

Table III. TAO inhibition by the derivatives with various alkyl chain.

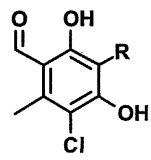

Compound	R	IC_{50} (nM)
4	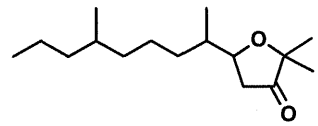	0.30
5	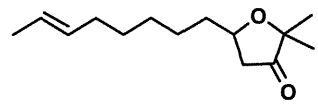	1.0
6	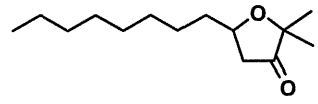	0.50

Table IV. TAO inhibition by the derivatives varying the side chain length.

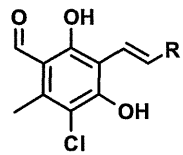

Compound	R	IC_{50} (nM)
7a	CH_3	100
7b	$CH_2CH_2CH_3$	3.8
7c	$CH_2CH_2CH_2CH_2CH_3$	0.70
7d	$CH_2CH_2CH_2CH_2CH_2CH_2CH_3$	0.38
7e	$CH_2CH_2CH_2CH_2CH_2CH_2CH_2CH_3$	0.38
7f	$CH_2CH_2CH_2CH_2CH_2CH_2CH_2CH_2CH_2CH_3$	0.45

hydroxyimino and methoxycarbonyl substitutions (**17** and **18**) (to 28 and 45 nM, respectively). These slightly larger substituted groups presumably hampered the access of inhibitors to the binding site due to their steric congestion.

The chloro-substituted compound **19** drastically decreased inhibitory activity (to a micromolar level), although the linker also was substituted to a linear alkyl chain. In contrast, the extent of the decrease in activity caused by the nitro-substituted and cyano-substituted derivatives (**20** and **21**) was moderate. Comparison of 1-position-substituted derivatives shows that the intramolecular hydrogen bond or the hydrogen-bonding donor activity of =**O** of the formyl group was crucial for strong inhibition (Tables VI and VII). The electronic property of the formyl group, or

Table V. TAO inhibition by the derivatives varying the bulkiness of the furanone ring portion.

Compound	Structure	IC_{50} (nM)
8	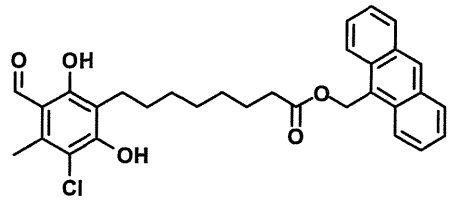	0.50
9	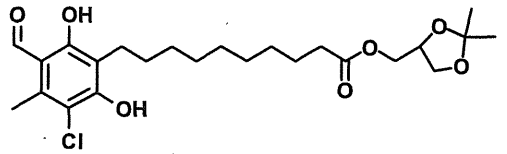	0.30
10	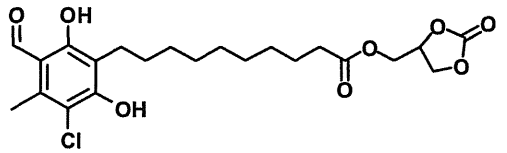	0.32
11	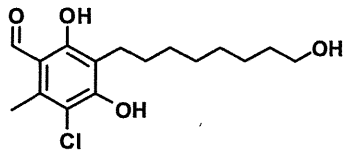	6.0
12	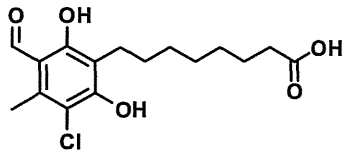	40
13	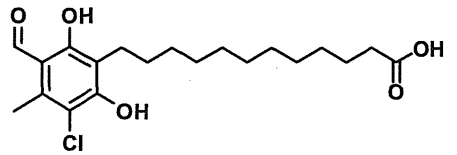	4.2

of the electron-withdrawing group, is not likely to be responsible for potent inhibition because the nitro-substituted derivative, which causes a stronger electron-withdrawing effect, exhibited a slightly decreased inhibitory activity. Surprisingly, the presence of the geranyl or Cα-carbonyl group in proximity to the aromatic ring appeared to compensate for the detrimental effect of the acetyl-substituted and the chloro-substituted derivatives (**15** versus **22** and **19** versus **23**), suggesting that the role of 1-formyl and/or 6-hydroxyl groups depends on the linker structure.

Next, 2- and 3-position derivatives were examined. Removal of 2-methyl (**25** and **26**) or 3-chloro (**27**) did not alter inhibitory activity, whereas removal of both moieties (**28**) decreased inhibitory activity (Table VIII). These four compounds all included a geranyl linker. The effects of 2- and 3-position substituents suggested that the major contribution of these functional groups for inhibition was not an electronic state affected by the 2-methyl and 3-chloro moieties, but a whole conformational preference, because the 2- and 3-position substituents did not diminish inhibitory activity when the compounds retained a geranyl moiety as a linker. In short, the 2- and/or 3-functional groups may affect the recognition of the geranyl moiety by the enzyme.

Finally, Table IX examines the role of AF's 4-hydroxyl group on TAO inhibition. The 4-methoxy substitution (**29**) resulted in low inhibitory activity, whereas the 4-hydrogen substitution (**30**) resulted in a complete loss of inhibition. This result suggests that the lone pair of electrons on the 4-hydroxyl's oxygen plays a role in the interaction of AF with the enzyme.

Table VI. TAO inhibition by 1-position substituted derivatives with a geranyl linker.

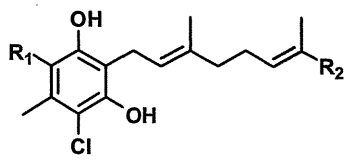

Compound	R1	R2	IC_{50} (nM)
14		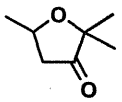	2.5
15		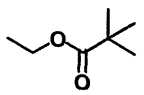	0.70
16		$-CH_3$	0.15
17		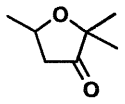	28
18		$-CH_3$	45

Table VII. TAO inhibition by 1-position substituted derivatives with a linear alkyl linker.

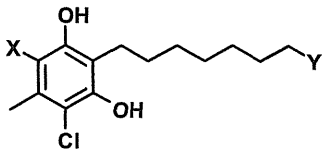

Compound	X	Y	IC_{50}(nM)
19	Cl—		10000
20	O_2N—		0.45
21	NC—	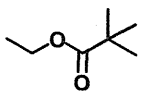	6.0
22		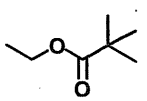	100

Table VIII. TAO inhibition by 2, 3-position substituted derivatives.

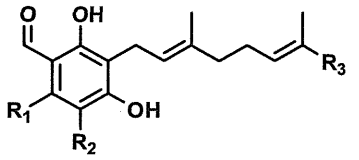

Compound	R1	R2	R3	IC_{50} (nM)
25	—H	—Cl	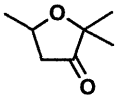	0.45
26	—H	—Cl	$-CH_3$	0.23
27	$-CH_3$	—H	$-CH_3$	0.50
28	—H	—H	$-CH_3$	38

Conclusion

This study revealed the structure–activity profiles as follows (Fig. 2). (i) The furanone ring is not essential for potent inhibition. (ii) One isoprene in proximity to the aromatic ring is recognized by the enzyme. (iii) Intramolecular hydrogen bonding and/or the hydrogen-bonding donor activity of the 1-formyl and 6-hydroxyl groups is responsible for direct interaction with the enzyme. (iv) The 2-methyl and/or 3-chloro groups contribute to the enzyme-bound conformation of the molecule. Notably, we have successfully designed and synthesized compound **24** (Table X), which exhibited more potent inhibitory activity than AF (0.06 nM). These AF derivatives and the present systematic structure–activity profiles provide important information about the reaction mechanism of TAO and AOXs. These data are expected to clarify the molecular mechanism of AF inhibition when considered in the context of the 3D structure of TAO (*17*, *18*).

SHAM and propyl gallate have been known as specific inhibitors of AOX since 1971 and 1980, respectively (*6*, *19*). Inhibitors have played a crucial role in the characterization of AOX, which has been recognized as the source of cyanide-insensitive, SHAM-sensitive oxygen consumption for years. The IC_{50} values of the two inhibitors against rTAO under our experimental conditions were 4 μM and 200 nM, respectively. Another class of AOX inhibitor, aurachin C, was reported in 1995 (*20*). Historical data did not identify any other inhibitors with inhibition higher than that of the lead compounds; however, some components of the inhibitors, such as the hydroxyl acetamide group of SHAM, were revealed to be responsible for inhibition (*7*). Accordingly, the intramolecular hydrogen bond and/or the hydrogen-bonding donor activity on the hydroxyl acetamide group might be analogous to that of AF.

For drug development, structural modification often is required to improve the pharmacological activity

Table IX. TAO inhibition by 4-position substituted derivatives.

Compound	Structure	IC_{50} (nM)
29	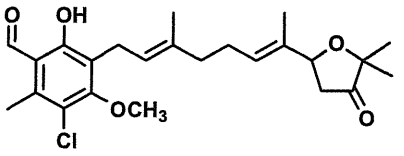	4.0
30	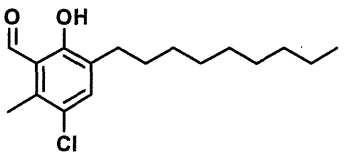	30% inhibition at 50 μM

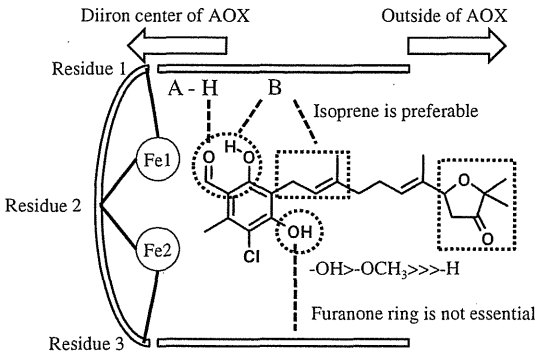

Fig. 2 Identification of pharmacophore of AF, which is a novel specific inhibitor of AOX. This figure illustrated the functional interaction between AF and AOX. The semicircular column and two rectangles represent the diiron catalytic centre of AOX and its substrate-binding cavity, in which AF interacts with AOX. The SAR study revealed that the hydrogen-bonding ability of 1-formyl and 6-hydroxyl group is responsible for potent inhibition of AOX (A–H, hydrogen-bonding donor; B, hydrogen-bonding acceptor). At 4-hydroxyl group, **-OH** is much preferable for potent inhibition rather than **–H**. Furanone ring is not essential for inhibition, suggesting this portion is oriented towards outside of AOX.

Table X. TAO inhibition by derivatives with various linker.

Compound	Structure	IC_{50} (nM)
23	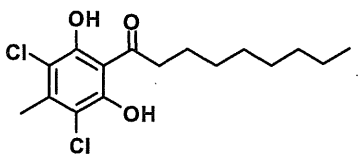	200
24	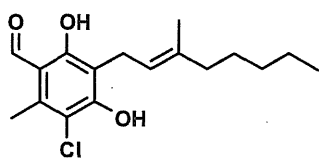	0.06

and the manufacturing process after absorption, distribution, metabolism, excretion and toxicity study. The identification of the pharmacophore and the elucidation of the interaction between drug and drug target could open the door to a novel drug development of AF for HAT. This study should be highly advantageous to change the necessary physical properties, including optimizing water solubility (for effective absorption *in vivo*) and designing a compound with a simple structure (to reduce synthetic costs). The information from the current SAR study is expected to contribute to the synthesis of a promising candidate.

Supplementary Data

Supplementary data are available at *JB online*.

Funding

This work was supported in part by Grant-in-aid for Young Scientists (B) 21 790 402 (to Y.K.), Grant-in-aid for Scientific Research (C) 23 590 484 (to K.S.), Creative Scientific Research Grant 18GS0314 (to K.K.), Grant-in-aid for Scientific Research on Priority Areas 18 073 004 (to K.K.) from the Japanese Society for the Promotion of Science and Programme for Promotion of Basic and Applied Researches for Innovations in Bio-oriented Industry (BRAIN) (to KK).

Conflict of interest

Not declared.

Acknowledgements

The authors gratefully thank Professor Anthony L. Moore (Sussex University, Brighton, UK) for the generous gift of *S. gutattum* AOX-encoding plasmid.

References

1. Chaudhuri, M., Ott, R.D., and Hill, G.C. (2006) Trypanosome alternative oxidase: from molecule to function. *Trends Parasit.* **22**, 484–491
2. Moore, A.L. and Siedow, J.N. (1991) The regulation and nature of the cyanide-resistant alternative oxidase of plant mitochondria. *Biochim. Biophys. Acta* **1059**, 121–140

3. Rhoads, D.M. and McIntosh, L. (1991) Isolation and characterization of a cDNA clone encoding an alternative oxidase protein of *Sauromatum guttatum*. *Proc. Natl Acad. Sci. USA* **88**, 2122–2126
4. McDonald, A.E. and Vanlerberghe, G.C. (2006) Origins, evolutionary history, and taxonomic distribution of alternative oxidase and plastoquinol terminal oxidase. *Comp. Biochem. Physiol. Part D Genomics Proteomics* **3**, 357–364
5. McDonald, A.E., Vanlerberghe, G.C., and Staples, J.F. (2009) Alternative oxidase in animals: unique characteristics and taxonomic distribution. *J. Exp. Biol.* **212**, 2627–2634
6. Lambowitz, A.M. and Slayman, C.W. (1971) Cyanide-resistant respiration in *Neurospora crassa*. *J. Bacteriol.* **108**, 1087–1096
7. Clarkson, A.B. Jr and Brohn, F.H. (1976) Trypanosomiasis: an approach to chemotherapy by the inhibition of carbohydrate catabolism. *Science* **194**, 204–206
8. Minagawa, N., Yabu, Y., Kita, K., Nagai, K., Ohta, N., Meguro, K., Sakajo, S., and Yoshimoto, A. (1997) An antibiotic, ascofuranone, specifically inhibits respiration and in vitro growth of long slender bloodstream forms of *Trypanosoma brucei*. *Mol. Biochem. Parasitol.* **84**, 271–280
9. Nihei, C., Fukai, Y., and Kita, K. (2002) Trypanosome alternative oxidase as a target of chemotherapy. *Biochim. Biophys. Acta* **1587**, 234–239
10. Nakamura, K., Fujioka, S., Fukumoto, S., Inoue, N., Sakamoto, K., Hirata, H., Kido, Y., Yabu, Y., Suzuki, T., Watanabe, Y., Saimoto, H., Akiyama, H., and Kita, K. (2010) Trypanosome alternative oxidase, a potential therapeutic target for sleeping sickness, is conserved among *Trypanosoma brucei* subspecies. *Parasitol. Int.* **59**, 560–564
11. Yabu, Y., Yoshida, A., Suzuki, T., Nihei, C., Kawai, K., Minagawa, N., Hosokawa, T., Nagai, K., Kita, K., and Ohta, N. (2003) The efficacy of ascofuranone in a consecutive treatment on *Trypanosoma brucei brucei* in mice. *Parasitol. Int.* **52**, 155–164
12. Yabu, Y., Suzuki, T., Nihei, C., Minagawa, N., Hosokawa, T., Nagai, K., Kita, K., and Ohta, N. (2006) Chemotherapeutic efficacy of ascofuranone in *Trypanosoma vivax*-infected mice without glycerol. *Parasitol. Int.* **55**, 39–43
13. Kido, Y., Sakamoto, K., Nakamura, K., Harada, M., Suzuki, T., Yabu, Y., Saimoto, H., Yamakura, F., Ohmori, D., Moore, A.L., Harada, S., and Kita, K. (2010) Purification and kinetic characterization of recombinant alternative oxidase from *Trypanosoma brucei brucei*. *Biochim. Biophys. Acta* **1797**, 443–450
14. Ito, K., Ogata, T., Kakizaki, Y., Elliott, C., Albury, M.S., and Moore, A.L. (2011) Identification of a gene for pyruvate-insensitive mitochondrial alternative oxidase expressed in the thermogenic appendices in *Arum maculatum*. *Plant Physiol.* **157**, 1721–1732
15. Williams, B.A., Elliot, C., Burri, L., Kido, Y., Kita, K., Moore, A.L., and Keeling, P.J. (2010) A broad distribution of the alternative oxidase in microsporidian parasites. *PLoS Pathog.* **6**, e1000761
16. Yoshida, T., Murai, M., Abe, M., Ichimaru, N., Harada, T., Nishioka, T., and Miyoshi, H. (2007) Crucial structural factors and mode of action of polyene amides as inhibitors for mitochondrial NADH-ubiquinone oxidoreductase (complex I). *Biochemistry* **46**, 10365–10372
17. Kido, Y., Shiba, T., Inaoka, D.K., Sakamoto, K., Nara, T., Aoki, T., Honma, T., Tanaka, A., Inoue, M., Matsuoka, S., Moore, A.L., Harada, S., and Kita, K. (2010) Crystallization and preliminary crystallographic analysis of cyanide-insensitive alternative oxidase from *Trypanosoma brucei*. *Acta Crystallogr. Sect. F Struct. Biol. Cryst. Commun.* **66**, 275–278
18. Moore, A.L. and Albury, M.A. (2008) Further insights into the structure of the alternative oxidase: from plants to parasites. *Biochem. Soc. Trans.* **36**, 1022–1026
19. Siedow, J.N. and Girvin, M.E. (1980) Alternative respiratory pathway: Its role in seed respiration and its inhibition by propyl gallate. *Plant Physiol.* **65**, 669–674
20. Hoefnagel, M.H., Wiskich, J.T., Madgwick, S.A., Patterson, Z., Oettmeier, W., and Rich, P.R. (1995) New inhibitors of the ubiquinol oxidase of higher plant mitochondria. *Eur. J. Biochem.* **233**, 531–537

Gene 516 (2013) 39–47

Contents lists available at SciVerse ScienceDirect

Gene

journal homepage: www.elsevier.com/locate/gene

Cloning and characterization of hypoxia-inducible factor-1 subunits from *Ascaris suum* — A parasitic nematode highly adapted to changes of oxygen conditions during its life cycle

Miho Goto [a], Hisako Amino [a], Mikage Nakajima [a], Naotoshi Tsuji [b], Kimitoshi Sakamoto [a,1], Kiyoshi Kita [a,*]

[a] Department of Biomedical Chemistry, Graduate School of Medicine, The University of Tokyo, 7-3-1 Hongo, Bunkyo-ku, Tokyo 113-0033, Japan
[b] Laboratory of Parasitic Diseases, National Institute of Animal Health, National Agriculture Research Organization, 3-1-5 Kannondai, Tsukuba, Ibaraki 305-0856, Japan

ARTICLE INFO

Article history:
Accepted 3 December 2012
Available online 23 December 2012

Keywords:
Ascaris suum
Hypoxia-inducible factor-1 (HIF-1)
Complex II
Hypoxia adaptation
Transcription factor
Fumarate respiration

ABSTRACT

The parasitic nematode *Ascaris suum* successfully adapts to a significant decrease in oxygen availability during its life cycle by altering its metabolic system dramatically. However, little is known about the regulatory mechanisms of adaptation to hypoxic environments in *A. suum*. In multicellular organisms, hypoxia-inducible factor-1 (HIF-1), a heterodimeric transcription factor composed of HIF-1α and HIF-1β subunits, is a master regulator of genes involved in adaptation to hypoxia. In the present study, cDNAs encoding HIF-1α and HIF-1β were cloned from *A. suum* and characterized. The full-length *A. suum hif-1α* and *hif-1β* cDNAs contain open reading frames encoding proteins with 832 and 436 amino acids, respectively. In the deduced amino acid sequences of *A. suum* HIF-1α and HIF-1β, functional domains essential for DNA-binding, dimerization, and oxygen-dependent prolyl hydroxylation were conserved. The interaction between *A. suum* HIF-1α and HIF-1β was confirmed by the yeast two-hybrid assay. Both *A. suum hif-1α* and *hif-1β* mRNAs were expressed at all stages examined (fertilized eggs, third-stage larvae, lung-stage larvae, young adult worms, and adult muscle tissue), and most abundantly in the aerobic free-living third-stage larvae, followed by a gradual decrease after infection of the host. *hif-1* mRNA transcription was not sensitive to the oxygen environment in either third-stage larvae or adult worms (muscle tissue), and was regulated in a stage-specific manner. High expression of *hif-1* mRNAs in third-stage larvae suggests its contribution to pre-adaptation to a hypoxic environment after infection of their host. Sequence analysis of 5′-upstream regions of mitochondrial complex II (succinate–ubiquinone reductase/quinol-fumarate reductase) genes, which show stage-specific expression and play an important role in oxygen adaptation during the life cycle, revealed that all subunits except for the adult-type flavoprotein subunit (Fp) possess putative hypoxia-responsive elements (HREs), suggesting that they are *hif-1* target genes.

1. Introduction

Multicellular organisms have developed cellular and systemic responses to low oxygen levels to meet metabolic demands. The parasitic nematode *Ascaris suum* experiences extreme changes in oxygen conditions during its life cycle and possesses unique metabolic mechanisms for survival in hypoxic environments within the host (Fig. 1) (Kita and Takamiya, 2002; Komuniecki and Harris, 1995; Sakai et al., 2012; Tielens and Van Hellemond, 1998).

A. suum fertilized eggs develop into infectious third-stage larvae (L3) under normoxic conditions outside of the host. After infection of the host, L3 larvae penetrate the intestinal wall and reach the lung (LL3), migrating through the liver and the heart. Afterwards, the larvae migrate back to the small intestine via the trachea and become adult worms under hypoxic conditions (Sakai et al., 2012; Takamiya et al., 1993).

To cope with decreased oxygen availability, *A. suum* alters its energy metabolism from a mammalian-type aerobic pathway in the larval stage to a unique anaerobic pathway, the phosphoenolpyruvate carboxykinase (PEPCK)-succinate pathway, in the adult stage (Kita et al., 2002). For the establishment of this anaerobic metabolism, quinol-fumarate reductase activity of mitochondrial respiratory chain complex II plays a crucial role to produce succinate as an end product. Complex II is generally composed of four peptides: the flavoprotein (Fp), the iron-sulfur cluster (Ip), the hydrophobic membrane-anchoring cytochrome *b* large subunit

Abbreviations: ARNT, aryl hydrocarbon receptor nuclear translocator; bHLH, basic helix-loop-helix; CAD, C-terminal activation domain; C-TAD, C-terminal transactivation domain; FIH, factor inhibiting HIF; HIF, hypoxia-inducible factor; HRE, hypoxia-responsive element; N-TAD, N-terminal transactivation domain; ODD, oxygen-dependent degradation domain; PAS, Per-Arnt-Sim; PHD, prolyl hydroxylase; SL1, spliced leader sequence 1; VHL, von Hippel–Lindau tumor suppressor.

* Corresponding author. Tel.: +81 3 5841 3526; fax: +81 3 5841 3444.
E-mail address: kitak@m.u-tokyo.ac.jp (K. Kita).
[1] Present address: Faculty of Agriculture and Life Science, Hirosaki University, 3 Bunkyo-cho, Hirosaki 036-8561, Japan.

0378-1119/$ – see front matter © 2012 Elsevier B.V. All rights reserved.
http://dx.doi.org/10.1016/j.gene.2012.12.025

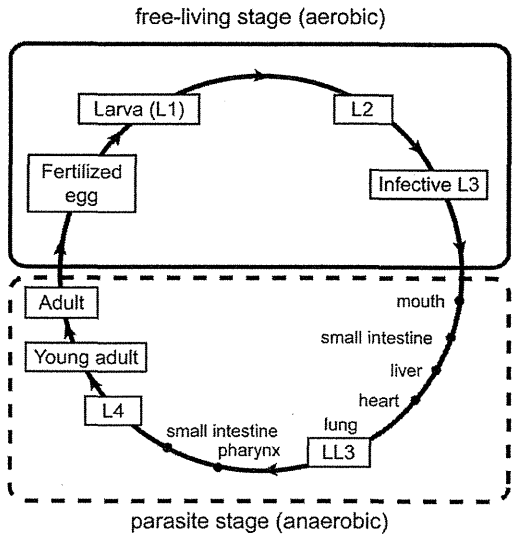

Fig. 1. Life cycle of *Ascaris suum*. Fertilized eggs embryonate and become infective third-stage larvae (L3) under normoxic conditions. L3 are ingested by the host and hatch in the small intestine. Afterwards, larvae migrate into the host organs (liver, heart, lung, pharynx), and finally reach the small intestine and develop into adult worms. In the small intestine, the oxygen concentration is lower than 5%.

(CybL), and the small (CybS) subunit, and functions as a succinate–ubiquinone reductase in the aerobic respiratory chain (Kita and Takamiya, 2002; Sakai et al., 2012). In a previous study, we showed that *A. suum* mitochondria express stage-specific isoforms of complex II (Amino et al., 2000, 2003; Saruta et al., 1995) and recently determined the structure of adult-type complex II (Shimizu et al., 2012). Fp and CybS subunits are distinct between the adult and larval forms, and expressions of these genes are controlled at the transcriptional level. However, the regulatory mechanisms responsible for the stage-specific expression of these genes have not been elucidated. Considering that *A. suum* does not have a respiratory or circulatory system, transcription factors are supposed to play important roles in sensing oxygen levels and induction of target genes.

In mammals, hypoxia-inducible factor-1 (HIF-1) is a key regulator of physiological responses to hypoxia. HIF-1 activates the transcription of numerous genes, including genes involved in erythropoiesis, angiogenesis, and glycolysis (Kaelin and Ratcliffe, 2008; Semenza, 2011). HIF-1 is a heterodimeric protein composed of HIF-1α and HIF-1β subunits, both of which are members of the bHLH-PAS (basic helix–loop–helix/Per-Arnt-Sim) family of transcription factors (Wang et al., 1995). The bHLH regions are known to be required for DNA binding and dimerization, and the PAS domains are suggested to be involved in dimerization, ligand binding, and other biological activities (Jiang et al., 1996; Zelzer et al., 1997). On the C-terminal side of the PAS domain, HIF-1α contains the oxygen-dependent degradation domain (ODD) and two transactivation domains, the N-terminal transactivation domain (N-TAD, spanning residues 531–575 of human HIF-1α) and the oxygen-regulated C-terminal transactivation domain (C-TAD, spanning residues 786–826 of human HIF-1α) (Jiang et al., 1997; Pugh et al., 1997). HIF-1β also possesses an activation domain named the C-terminal activation domain (CAD) (Jain et al., 1994).

Under normoxic conditions, HIF-1α is targeted for polyubiquitination and proteosomal degradation through the oxygen-dependent hydroxylation of the conserved proline residues in the ODD by HIF prolyl hydroxylases (PHDs) and interaction with the von Hippel–Lindau tumor suppressor protein (VHL) (Epstein et al., 2001; Ivan et al., 2001; Jaakkola et al., 2001). The transcriptional activity of HIF-1α is also regulated by hydroxylation of the conserved asparagine residue in its C-TAD by factor inhibiting HIF (FIH) (Lando et al., 2002a,b). In contrast, prolyl hydroxylation and subsequent degradation of HIF-1α is inhibited under hypoxia. This permits HIF-1α to translocate to the nucleus, dimerize with HIF-1β, and activate the expression of target genes, which act to increase oxygen delivery or implement metabolic adaptation (Kallio et al., 1998).

HIF-1 homologs have been identified and characterized in a diverse array of multicellular organisms, and its function is also required for hypoxic adaptation in the free-living nematode, *Caenorhabditis elegans* (Jiang et al., 2001a; Powell-Coffman et al., 1998). The ubiquitous presence and diverse functions of HIF-1 suggest that it also plays crucial roles in hypoxic adaptation in *A. suum*.

In the present study, cDNAs for HIF-1α and HIF-1β homologs of *A. suum* were cloned by RT-PCR using degenerate primers. The functional interaction between *A. suum* HIF-1α and HIF-1β was confirmed by yeast two-hybrid assays. Furthermore, *hif-1* mRNA expression levels were examined in the aerobic free-living stages (fertilized eggs, L3 larvae) and the anaerobic parasitic stages (LL3, young adult worms, and adult muscle tissue). In addition, nucleotide sequences of 5′-upstream regions of complex II genes were determined and searched for hypoxia-responsive elements (HREs).

2. Material and methods

2.1. Experimental animals

Adult *A. suum* worms were collected from the intestines of infected pigs in a slaughterhouse in Tokyo, Japan. Adult worms were dissected to obtain muscle and uterine tissue. Fertilized eggs were isolated from uterine tissue of adult worms, which had been stored in 0.5 M sodium hydroxide at 4 °C, by homogenization and centrifugation and allowed to develop to L3 aerobically as previously described (Iwata et al., 2008). For preparation of LL3 larvae and young adult worms, pigs were orally infected with eggs containing L3 larvae (approximately 10^5 and 10^4 eggs per pig, respectively), and worms were collected from the lungs and small intestine of the pig 7 days and 38 days after ingestion, respectively (Islam et al., 2006). This study was carried out in strict accordance with the recommendations of the Guide for the Care and Use of Laboratory Animals of the National Institutes of Animal Health. The protocol was approved by the Committee of the Ethics of Animal Experiments of the NIAH (Permit Number: 07-29, 08-023, 09-019, 10-007). All surgeries were performed under sodium pentobarbital anesthesia, and all efforts were made to minimize the animals' suffering. Whole bodies of the *A. suum* worms were used for total RNAs extraction, except that muscle tissue, which comprises the most part of an adult worm, was used as the representative of a whole body of an adult worm to avoid the interfusion of eggs existing in female adult genital tracts. Each sample was immediately frozen with liquid nitrogen and stored at −80 °C until use.

2.2. Cloning of *A. suum hif-1α and hif-1β cDNAs*

Frozen muscle of an adult *A. suum* worm was pulverized in a mortar and pestle containing liquid nitrogen, and total RNAs were extracted by the acid guanidinium-phenol-chloroform (AGPC) method (Chomczynski and Sacchi, 1987). Poly(A)$^+$ RNAs were purified from total RNAs using an Oligo (dT)-Cellulose column (GE Healthcare). For the cloning of the partial sequences of *hif-1* cDNAs and the following 5′RACE, cDNA was synthesized with random primers $(N)_6$ (Takara) using ReverTraAce (Toyobo) as a reverse transcriptase. For the 3′ RACE, the oligo (dT) primer P-383 was used (Table 1).

Partial sequences corresponding to the bHLH and the PAS domains of nematode *hif-1α* were obtained by a TBLASTN search of the Nematode.net website (http://www.nematode.net/) and TIGR database (http://www.jcvi.org/) using the amino acid sequences of *C. elegans hif-1* (*C. elegans hif-1α*) (GenBank ID: NM_001028722) as a query. The degenerate primers were designed based on the conserved amino acid sequences

Table 1
Primers used in this study.

P-80	(F)	5′-GGTTTAATTACCCAAGTTTGAG-3′
P-383	(R)	5′-$(T)_{18}$ AAGGACGCCGGCGCTTAAGAAGGTCAA-3′
P-385	(R)	5′-GAATTCGCGGCCGCAG-3′
P-746	(F)	5′-GNATGGCNGTNTCNCA(C/T)ATG-3′
P-747	(R)	5′-A(A/G)(A/G)AANCCAT(C/T)NGC(A/C/T)GC(C/T)TC-3′
P-753	(F)	5′-CTATCCGTGGTACGTCTCAG-3′
P-754	(R)	5′-GTATTAGGTGCTTCAGTTCTTGG-3′
P-755	(R)	5′-CTGGAAGAATTCGCGGC-3′
P-758	(F)	5′-GACAGACCAAGAACTGAAGC-3′
P-759	(R)	5′-GAGACGTACCACGGATAGC-3′
P-1900	(F)	5′-CGCCATGGCAATGTCAAAGTATGCACGGAATG-3′
P-1904	(R)	5′-AAGGATCCTAACAAGACCGTCTTTGAG-3′
P-2086	(F)	5′-CC(T/A)ATTGTTGA(A/C/T)GAAG-3′
P-2087	(F)	5′-TA(C/T)(C/T)T(C/T/A)GGA(C/T)T(T/A)AC(A/G)CA(A/G)-3′
P-2090	(R)	5′-CAT(A/G)TC(G/A)(C/T)A(A/T/G)GT(A/G)TG-3′
P-2103	(R)	5′-ATC(T/G)GC(T/C)GGAT(G/A)(T/A)A(T/C)(T/C)AA-3′
P-2132	(R)	5′-CACAAATTCCTTCAGAGATCG-3′
P-2133	(F)	5′-CGTGGAAGAAATCTCAACCTC-3′
P-2134	(R)	5′-GAGGTTGAGATTTCTTCCACG-3′
P-2135	(F)	5′-CAAGAGTGCTGAAATCCCTAAC-3′
P-2582	(F)	5′-CGATCTCTGAAGGAATTTGTG-3′
P-2951	(F)	5′-CATCGAATTCATGATGGCCGATCATGGTGGTG-3′
P-2953	(R)	5′-GTCGCTGAGCTCCTATGCCGCCGAAGTATCTCTACG-3′

Abbreviations: F, forward; R, reverse; N, A, C, G, or T.
The underlined sequences indicate the restriction sites: CCATGG, *Nco*I; GGATCC, *Bam*HI; GAATTC, *Eco*RI; GAGCTC, *Sac*I.

among nematodes: *C. elegans*, *Brugia malayi* (TIGR database ID: 14615.m00142), and *Strongyloides ratti* (GenBank ID: CD523815). The nucleotide sequences and positions of the primers used for cloning of *A. suum hif-1α* and *hif-1β* are shown in Table 1 and Fig. 2, respectively. The first PCR was performed using a forward primer designed based on the spliced leader sequence 1 (SL1) of nematodes (Nilsen et al., 1989), P-80, and a reverse degenerate primer P-2103. The first PCR product was used as a template for the nested PCR with degenerate primers, P-2086 and P-2103. Further PCR amplification was carried out from the nested PCR product with degenerate primers, P-2087 and P-2090. PCR was performed under low stringent thermal conditions consisting of 30 cycles of 90 °C for 30 s, 42 °C for 1 min, 72 °C for 1 min. The resulting PCR product with the expected size (360 bp) was inserted into the pGEM-T plasmid (Promega) and sequenced. Specific primers for 5′ and 3′-RACE were designed from the nucleotide sequence of the subcloned fragment. For 5′-RACE, the first PCR was performed with SL1 primer P-80 and a specific primer P-2134. Nested PCR was carried out using P-80 and a specific primer P-2132. For 3′-RACE, the first PCR was carried out using a specific primer P-2133 and an adapter primer P-755. Nested PCR was carried out with a specific primer P-2135 and an adapter primer P-385.

For cloning of partial sequences of *hif-1β*, degenerate primers were designed based on the conserved amino acid residues corresponding to the bHLH regions of *hif-1β* of various organisms: *Homo sapiens* (GenBank ID: NM_001668), *Bos taurus* (GenBank ID: AB053954), *Rattus norvegicus* (GenBank ID: NM_012780), *Mus musculus* (GenBank ID: BC012870), *Gallus gallus* (GenBank ID: AF348088), *Xenopus laevis* (GenBank ID: AY036894), *Drosophila melanogaster* (GenBank ID: AF154417), and *C. elegans* (GenBank ID: AF039569). The PCR reaction was performed with 30 cycles of 94 °C for 45 s, 53 °C for 30 s, 72 °C for 90 s using degenerate primers P-746 and P-747. The PCR product with the expected size (130 bp) was cloned into the pGEM-T plasmid (Promega) and sequenced. 5′RACE was performed with SL1 primer P-80 and a specific primer P-754. Nested PCR was carried out using P-80 and a specific primer P-759. For 3′RACE, first PCR was carried out using specific primers P-753 and P-755. Nested PCR was carried out with specific primers P-758 and P-385.

2.3. Construction of the prey and bait plasmids for yeast two-hybrid assay

A. suum hif-1α and *hif-1β* cDNAs were fused to the GAL4 activation domain of the prey plasmid pGADT7 (Clontech) and the GAL4 DNA-binding domain of the bait plasmid pGBKT7 (Clontech), respectively. DNA fragments of *A. suum hif-1α* and *hif-1β* were amplified by PCR using *Pfu* turbo DNA polymerase (Stratagene) and pGEM-T (*hif-1α*) or pGEM-T (*hif-1β*) plasmid DNA as a template with primers in which restriction sites were incorporated. Primers P-2951 and P-2953 were used for *hif-1α* amplification, while primers P-1900 and P-1904 were used for *hif-1β* amplification. Nucleotide sequences of the primers are shown in Table 1.

PCR products were digested with the appropriate restriction enzymes and inserted into plasmids with T4 DNA ligase (Invitrogen).

2.4. Yeast two-hybrid assay

The interaction between recombinant *A. suum* HIF-1α and HIF-1β was analyzed by the yeast two-hybrid assay using MATCHMAKER GAL-4 Two-Hybrid Systems (Clontech) according to the manufacturer's instructions. The prey plasmid pGADT7-GAL4-HIF-1α expressing a fused protein of HIF-1α and the GAL4 activation domain, and the bait plasmid pGBKT7-GAL4-HIF-1β expressing a fused protein of HIF-1β and the GAL4 DNA binding domain, were introduced into competent AH109 yeast cells by the polyethylene glycol (PEG)/lithium acetate-based method. Transformants were plated on synthetic dropout (SD) agar plates lacking leucine/tryptophan or adenine/histidine/leucine/tryptophan and incubated at 30 °C until the appearance of colonies.

2.5. Real-time PCR

Transcript levels of *A. suum hif-1α* and *hif-1β* mRNAs at different developmental stages were determined by real-time PCR. Triplicate samples of fertilized eggs, L3, and adult muscle tissue, and single samples of LL3 and young adult worms were pulverized in a mortar and pestle containing liquid nitrogen, and total RNAs were extracted using Trizol LS Reagent (Invitrogen). Total RNAs of each sample were treated with

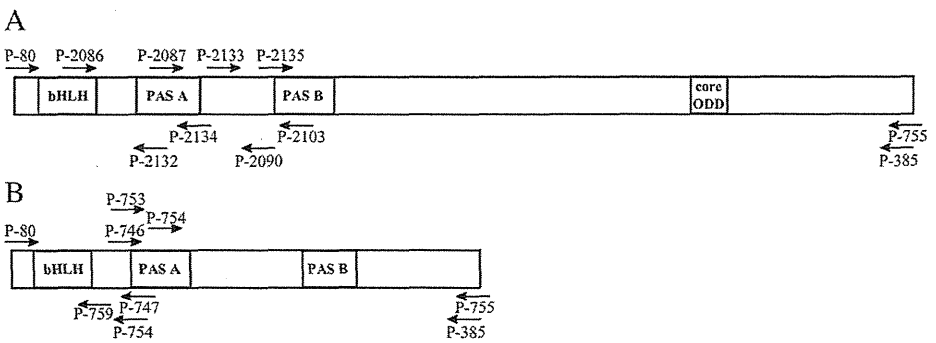

Fig. 2. Positions of primers designed for RT-PCR of (A) *A. suum* HIF-1α and (B) *A. suum* HIF-1β.

DNase I (Invitrogen) and quantified using the RiboGreen reagent (Molecular Probes) with a spectrofluorometer (Jasco FP-6300). Equal amounts (1 μg) of total RNAs were used as templates for reverse transcription with a SuperScript VILO synthesis kit (Invitrogen). Real-time PCR was carried out on a LightCycler (Roche) using QuantiTect SYBR Green PCR Master Mix (Qiagen). The PCR reaction was performed with 30 cycles of 94 °C for 15 s, 55 °C for 30 s, 72 °C for 10 s. Primers P-2582 and P-2134 were used for *hif-1α*, and P-753 and P-754 were used for *hif-1β*. Nucleotide sequences of the primers are shown in Table 1.

2.6. Normoxic and hypoxic exposure of A. suum worms

L3 and adult worms were incubated under either normoxic or hypoxic conditions for 16 hr at 37 °C. For hypoxic exposure, L3 and adult worms were soaked in phosphate buffered saline (PBS) and placed into the GasPak System (BBL). Parallel to hypoxic exposure, worms were soaked in PBS and placed into an incubator in the presence of air. According to the manufacturer's instruction for GasPak System, oxygen concentration decreases to less than 0.1% within 90 min, and the establishment of this condition was confirmed using a methylene blue indicator purchased from BBL. Total RNAs were extracted from triplicate samples of adult muscle and a single sample of L3.

2.7. Sequence analysis of 5′-upstream regions of complex II genes

Approximately 2 kb 5′-upstream sequences of the coding start sites of *A. suum* complex II subunit genes were analyzed. Genomic clones containing the corresponding regions were isolated from a lambda Fix II genomic library of *A. suum* by plaque hybridization using a digoxygenin (DIG)-labeled nucleotide probe. Each fragment was inserted into the pZErO-2 plasmid (Invitrogen) and sequenced (Operon).

3. Results

3.1. Cloning of A. suum hif-1α and hif-1β cDNAs

To obtain partial sequences of *A. suum hif-1α* and *hif-1β* cDNAs by RT-PCR, degenerate primers were designed based on conserved amino acid sequences corresponding to the bHLH and the PAS domains of vertebrate and invertebrate HIF-1s. Partial sequences of *A. suum hif-1α* cDNA were not amplified using these primers, while those of *hif-1β* were obtained. Then, the nematode EST database was searched for *hif-1α* homologs using amino acid sequences of *C. elegans* HIF-1 as a query, and degenerate primers were redesigned based on the conserved regions among nematode species: *C. elegans*, *S. ratti*, and *B. malayi*. As a result, partial sequences of *A. suum hif-1α* cDNA were amplified. Finally, by performing 5′RACE using the nematode spliced leader sequence SL1, and 3′RACE, the full-length *A. suum hif-1α* and *hif-1β* cDNAs were obtained.

The full-length *A. suum hif-1α* cDNA consists of 2861 bp, which contains 234 bp of 5′UTR, 2499 bp of open reading frame encoding 832 deduced amino acid residues, and 128 bp of 3′UTR including a polyA signal sequence (GenBank ID: AB520828). An alignment of the conserved N-terminal amino acid sequences of *A. suum* HIF-1α with those of *B. malayi*, *C. elegans*, *Daphnia magna*, *X. laevis*, and *H. sapiens* is shown in Fig. 3A. *A. suum* HIF-1α exhibits high sequence conservation in the bHLH, PAS-A, and PAS-B domains, which have 76%, 67%, and 59% identities to those of *C. elegans* HIF-1, respectively. In the C-terminal side of the PAS B domain, the core sequence of the ODD, which is essential for prolyl hydroxylation and generally contains an LXXLAP motif (X indicates any amino acid and P indicates the hydroxylacceptor proline) (Huang et al., 2002), was found (Fig. 3B). However, homologous sequences corresponding to neither the N-TAD nor the C-TAD were identified (Fig. 3C).

The full-length *A. suum hif-1β* cDNA consists of 1558 bp, which contains 50 bp of 5′UTR, 1308 bp of open reading frame encoding a deduced 435 amino acid residues, and 200 bp of 3′UTR including a polyA signal sequence (GenBank ID: AB520829). An alignment of the amino acid sequences of the full-length *A. suum* HIF-1β with those of other organisms is shown in Fig. 4A. The bHLH, PAS-A, and PAS-B domains are highly conserved in *A. suum* HIF-1β and show 96%, 70%, and 47% identities to those of *C. elegans* AHA-1 (*C. elegans* HIF-1β), respectively. On the other hand, the C-terminus of *A. suum* HIF-1β is significantly shorter than those of other organisms, and the CAD was not found (Fig. 4B).

3.2. Interaction between A. suum HIF-1α and HIF-1β

As described in previous reports on *H. sapiens* and *C. elegans* HIF-1s, canonical HIF-1 consists of HIF-1α and HIF-1β subunits, and their dimerization is essential for their binding to HREs (Jiang et al., 2001a; Kallio et al., 1997). To determine whether *A. suum* HIF-1 forms a similar complex, the interaction between *A. suum* HIF-1α and HIF-1β was analyzed by yeast two-hybrid assays. Yeast strain AH109 co-transformed with both plasmids pGADT7-GAL4-HIF-1α and pGBKT7-GAL4-HIF-1β grew on selective medium lacking adenine, histidine, leucine, and tryptophan, while cells expressing either pGADT7-GAL4-HIF-1α or pGBKT7-GAL4-HIF-1β formed no colonies (Fig. 5). The specific interaction between *A. suum* HIF-1α and HIF-1β indicates that these two proteins are binding partners.

3.3. Stage-specific expression of hif-1α and hif-1β mRNAs

A. suum fertilized eggs develop to L3 worms under normoxic conditions (150–160 mm Hg), while adult worms inhabit a hypoxic environment (0–10 mm Hg) (Kita and Takamiya, 2002; Takamiya et al., 1993). In order to determine if there is a regulatory relationship between *hif-1* expression and the oxygen conditions in different habitats, transcript levels of *hif-1α* and *hif-1β* were examined in the aerobic free-living stages and the anaerobic parasite stages by real-time PCR. As shown in Fig. 6, both *hif-1* mRNAs were expressed at all stages and most abundantly in aerobic free-living L3. *hif-1α* and *hif-1β* mRNA levels in L3 were 8-fold and 6-fold higher than those in adult muscle, respectively. In the parasite stages, both *hif-1* mRNAs gradually decreased as worms developed. In fertilized eggs, *hif-1α* mRNA expression was 6-fold higher than that of adult muscle, while *hif-1β* mRNA expression was slightly higher (1.2-fold) than that of adult muscle.

In hypoxia-tolerant organisms such as the mole rat *Spalax*, HIF-1α expression is induced by hypoxic exposure not only at the post-transcriptional but also at the transcriptional level (Rahman and Thomas, 2007; Shams et al., 2004). Although there is a report that the perienteric fluid of the adult worm was kept hypoxic even under normoxic conditions due to existence of oxygen-avid hemoglobin, it was suggested that at least some degree of oxygen diffused through muscle walls (Minning et al., 1999). In order to assess the effect of oxygen conditions on *hif-1* expression, transcript levels of *hif-1* mRNAs were compared between normoxia- and hypoxia-exposed L3 and adult worms (muscle tissue) by real-time PCR.16-hours incubation was adopted, because 12-hour and 16-hour exposures made no difference in expression of hypoxia-related genes in our preliminary study. Consequently, no significant difference was observed in either of the two groups as shown in Fig. 7.

3.4. Sequence analysis of 5′-upstream regions of A. suum complex II genes

The mammalian HIF-1 binds to specific DNA sequences called the HREs, which contain the sequence 5′-RCGTG (Wang and Semenza, 1993). Similarly, in *C. elegans*, a survey of the sequences 200–2000 bp 5′ upstream of the predicted translational start sites showed that the sequence 5′-TACGTG was present in 46% of *hif-1*-dependent genes (Shen et al., 2005).

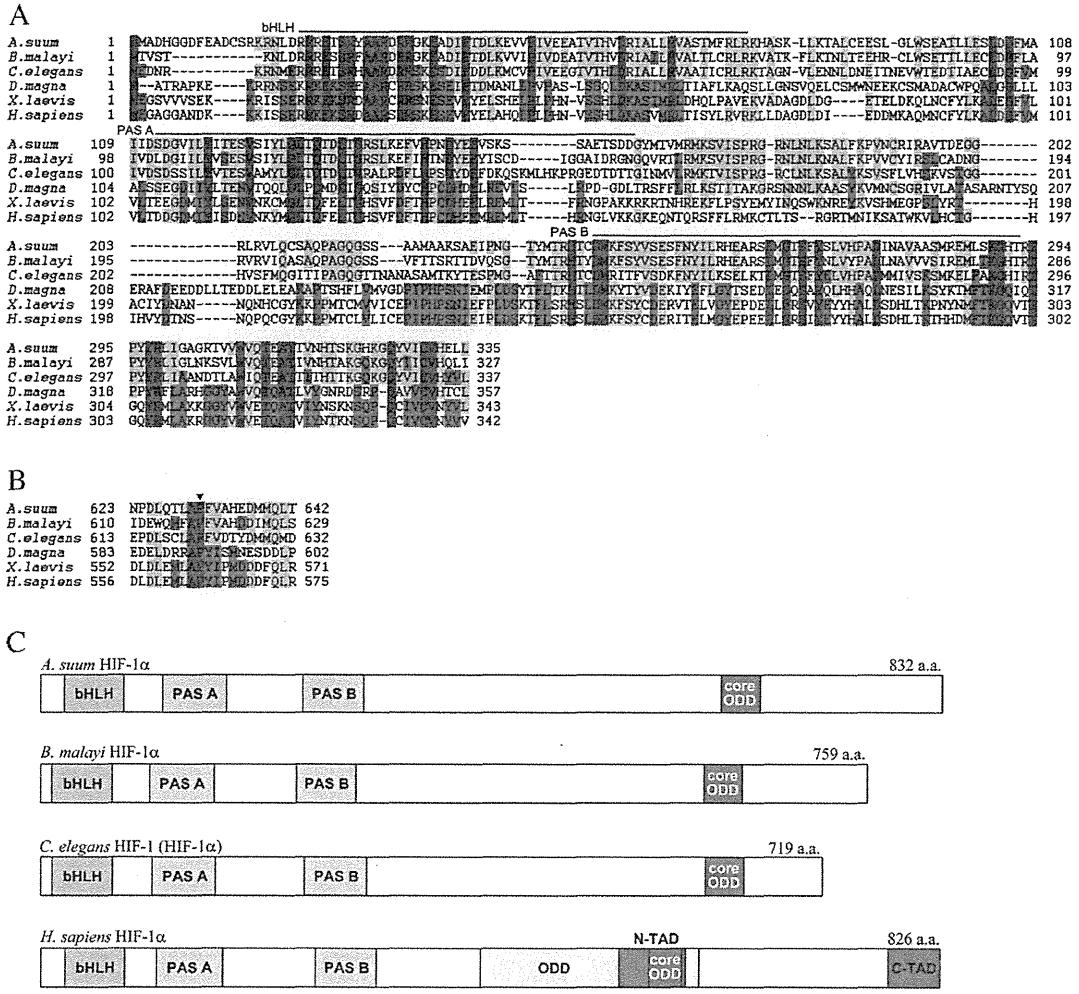

Fig. 3. Alignment of the deduced amino acid sequences of *A. suum* HIF-1α with homologs of other organisms. Amino acid sequences are designated by single-letter codes and numbered. Identical amino acid residues shared by all six species are highlighted in blue. Conserved residues in three species are shaded in green or pink whether including *A. suum* or not. Dashes indicate gaps introduced to facilitate alignment. (A) Conserved N-terminal amino acid sequences of HIF-1α. Black bars represent the bHLH, PAS-A, and PAS B domains. (B) Amino acid sequences around the core sequences of the ODD. The conserved proline residues are indicated by an arrowhead. (C) Domain structures of HIF-1α of nematodes (*A. suum*, *B. malayi*, and *C. elegans*) and humans.

Since the Fp and CybS subunits of *A. suum* complex II are expected to be target genes of HIF-1, nucleotide sequences of 5′-upstream regions of these genes were determined and searched for putative HREs on the assumption that the HRE motif is conserved between *C. elegans* and *A. suum*. Consequently, all the subunits except for adult-type Fp were found to possess putative HREs in their 5′-upstream regions (Fig. S1). Nucleotide sequences are available in the DDBJ/EMBL/GenBank databases under accession numbers AB626613–AB626618.

4. Discussion

Certain hypoxia-tolerant organisms are known to alter their metabolic pathways from aerobic-type to anaerobic-type in parallel with changes in the oxygen environment (Kita et al., 1997; Komuniecki and Harris, 1995; Tielens and Van Hellemond, 1998). *A. suum* is the biochemically best-characterized model organism among parasitic helminths and exhibits a prominent transition in carbohydrate metabolism during development. However, nothing is known about the regulatory mechanisms by which *A. suum* senses environmental oxygen concentrations and activates transcription of responsible genes for adaptation to hypoxia. The present study is the first report of cloning and characterization of *hif-1α* and *hif-1β* cDNAs from the parasitic helminth.

4.1. Cloning of *A. suum hif-1α* and *hif-1β* cDNAs

The predicted amino acid sequences of both *A. suum* HIF-1α and HIF-1β showed high levels of sequence conservation across phyla in the N-terminal regions from the bHLH domains to the PAS domains. During the preparation of this manuscript, the transcriptome information of *A. suum* was released (Wang et al., 2011), in which both HIF-1α and HIF-1β were annotated (GenBank ID: JI166617.1 and JI171286.1, respectively), and the deduced amino acid sequences of HIF-1α were exactly same as our result except for one amino acid at residue 754 (valine in our result and isoleucine in the transcriptome data). The core sequences of the ODD containing the LXXLAP motif are conserved in *A. suum* HIF-1α; in addition, homologous genes encoding PHD and VHL are found in the transcriptome analysis of *A. suum* (GenBank ID: JI165998.1 and JI165450.1, respectively) (Wang et al., 2011), supporting the hypothesis that *A. suum* HIF-1α is regulated by oxygen-dependent prolyl hydroxylation of the LXXLAP motif and functions as oxygen sensor as reported for *C. elegans* and humans (Epstein et al., 2001; Jaakkola et al., 2001). Our HIF-1β amino acid sequences were identical to the annotated HIF-1β from the transcriptome analysis between residues 1–433; however, they were 28 amino acids shorter in the N-terminus and 3 amino acids longer in the C-terminus. Because our HIF-1β sequences

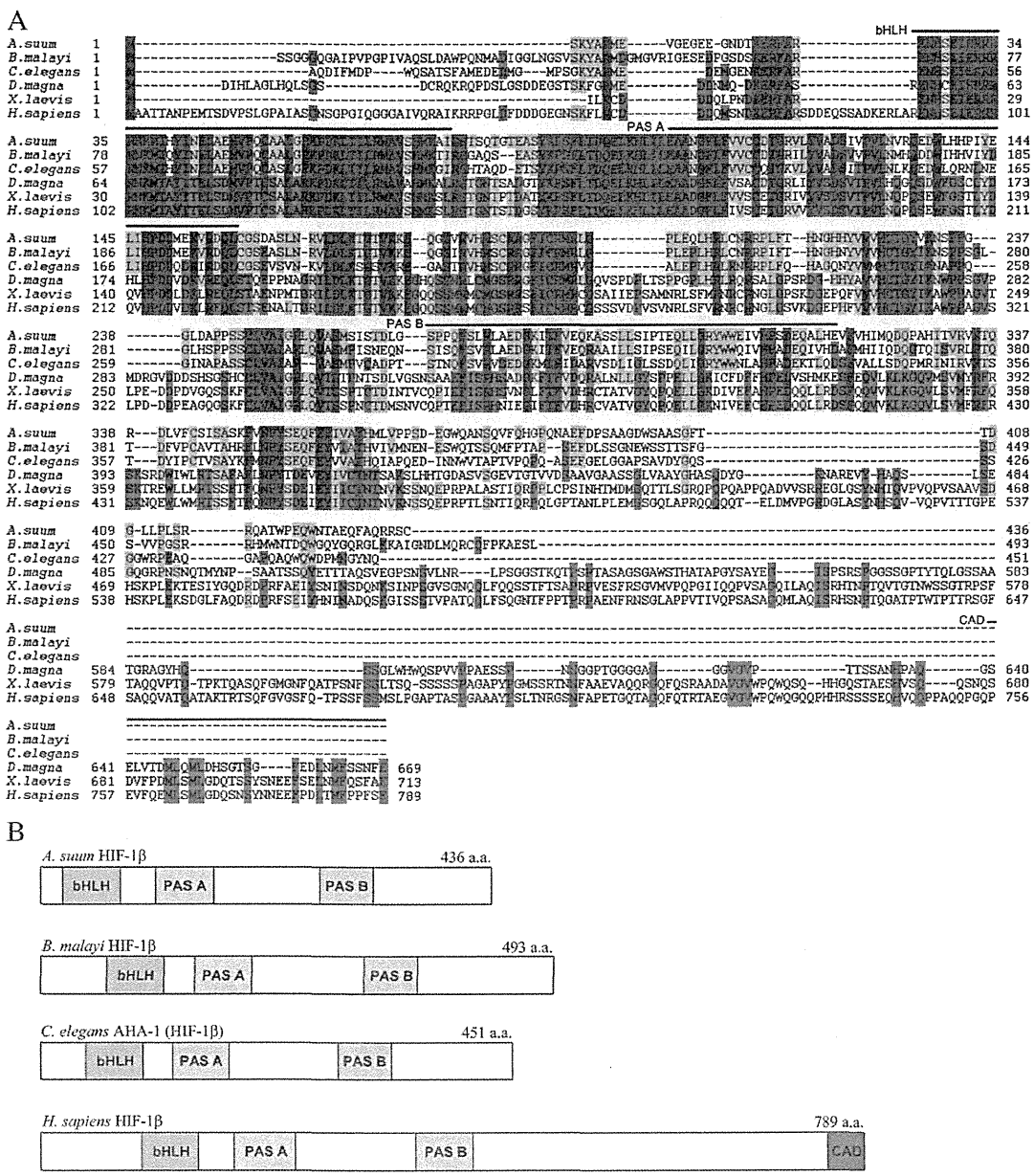

Fig. 4. (A) Alignment of the deduced amino acid sequences of *A. suum* HIF-1β with homologs of other organisms. Amino acid sequences are designated by single-letter codes and numbered. Identical amino acid residues shared by all six species are highlighted in blue. Conserved residues in three species are shaded in green or pink whether including *A. suum* or not. Dashes indicate gaps introduced to facilitate alignment. Black bars represent the bHLH, PAS-A, PAS B, and CAD domains. (B) Domain structures of HIF-1β of nematodes (*A. suum*, *B. malayi*, and *C. elegans*) and humans.

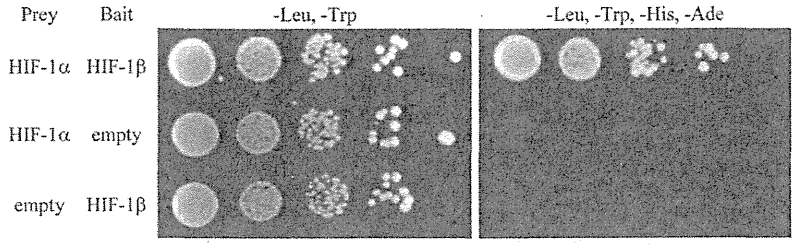

Fig. 5. Analysis of the interaction between *A. suum* HIF-1α and HIF-1β by yeast two-hybrid assays. Serial dilutions of yeast strains transformed with the indicated constructs were grown on plates lacking Leu and Trp as a control (left) and lacking Leu, Trp, His, and Ade (right).

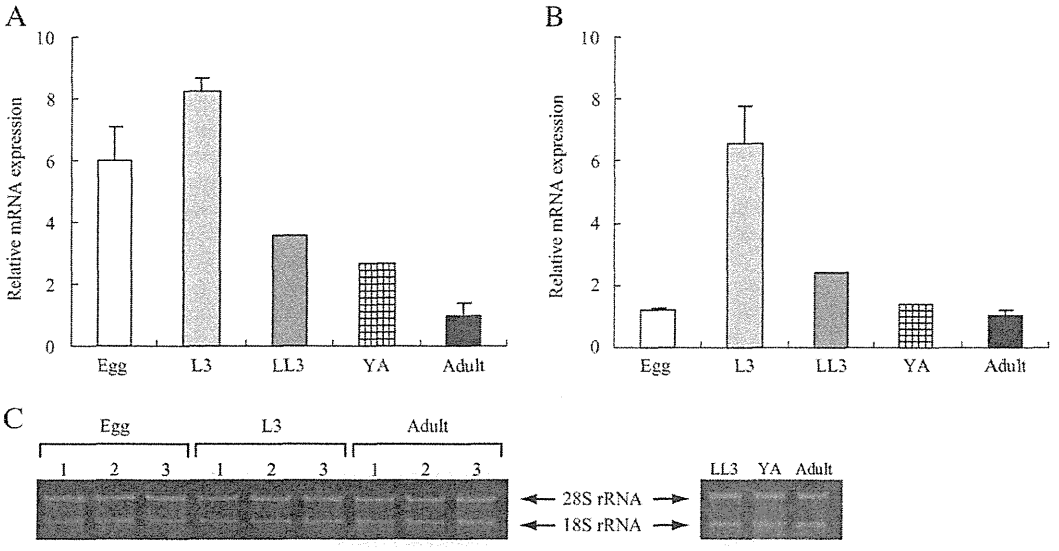

Fig. 6. Expression levels of *hif-1* mRNA at different developmental stages in *A. suum*. The ratios of mRNA levels in each sample to those in adult muscle are shown (A, *hif-1α* and B, *hif-1β* mRNA levels. C, 1 μg of total RNAs from each stage used for reverse transcription). Values are the means of three experiments ± SD. In fertilized eggs, the *hif-1α* level was 6-fold higher than that of adult muscle, while *hif-1β* showed only a slight difference between these two stages. *hif-1α* and *hif-1β* levels in L3 were 8-fold and 6-fold higher than those in adult muscle, respectively. In anaerobic parasite stages, both levels were gradually decreased during development.

contained both SL1 sequences and polyA signal sequences, it appears to exist as a processed transcript in adult worms, although there may be several splicing variants. In addition to the conservation of functionally important domains, the yeast two-hybrid assay indicated that *A. suum* HIF-1α and HIF-1β form a complex. These results strongly suggest that *A. suum* HIF-1α and HIF-1β dimerize and play an important role in adaptation to hypoxia.

In contrast to the sequence conservation in the N-terminal regions, *A. suum* HIF-1 subunits exhibited remarkable diversity in the C-terminal region of the PAS domains, except for the core sequences of the ODD in HIF-1α. *A. suum* HIF-1β is approximately 250 amino acids shorter than vertebrate HIF-1βs at the C-termini, and lacks the CAD. This property is commonly observed in other nematodes such as *B. malayi* and *C. elegans*. Because the CAD is conserved not only in vertebrates but also in arthropods, such as *D. melanogaster* and *D. magna* (Sonnenfeld et al., 1997; Tokishita et al., 2006), the CAD could have been evolutionarily lost from a common ancestor of nematode species. However, substantial induction of hypoxia-responsive genes occurs in *C. elegans* lacking the CAD (Epstein et al., 2001). Similarly, in mammals, the CAD is dispensable for transcriptional activation of both hypoxia-responsive and dioxin-responsive genes (Beischlag et al., 2004; Li et al., 1996). From these observations, *A. suum* HIF-1β lacking the CAD is suggested to be capable of inducing HIF-1 target genes.

Neither the N-TAD nor the C-TAD is identified in the C-terminal region of nematode HIF-1αs, and nematodes lack homologs of FIH-1, which in mammals catalyzes hydroxylation of a conserved asparagine residue in the C-TAD and represses HIF-1 transactivation in normoxia. This observation is consistent with a previous report claiming that no species have been identified wherein the C-TAD or FIH-1 is retained without the other (Hampton-Smith and Peet, 2009). Because the more phylogenetically basal *Acropora millepora* (*Cnidaria*) possesses functional FIH-1/C-TAD signaling (Hampton-Smith and Peet, 2009), nematodes appear to have lost the FIH-1 gene and the C-TAD from a common ancestor of nematode species, although their biological significance remains to be elucidated. Even compared with *B. malayi* and *C. elegans* HIF-1αs, the C-terminal region of *A. suum* HIF-1α is distinct in its length and shows no sequence similarity. In mammals, unlike the CAD, both the N-TAD and the C-TAD are essential for the recruitment of coactivators CBP/p300, SRC-1, and transcription intermediary factor 2 (TIF-2) (Gu et al., 2001; Lando et al., 2002a). While the C-TAD contributes to the regulation of most HIF target genes and is the predominant transactivation domain, the N-TAD confers HIF target gene specificity (Hu et al., 2007). The unique features of the C-terminal region of *A. suum* HIF-1α may shed light on new mechanisms of activation of HIF-1 and the regulation of target gene specificity.

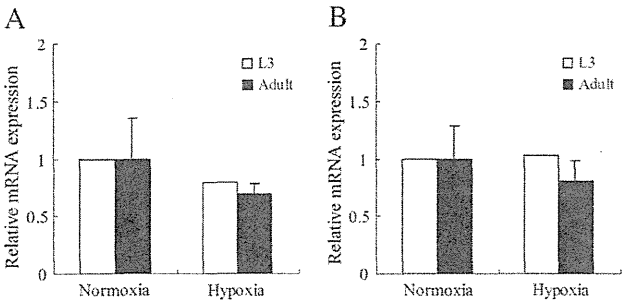

Fig. 7. Effects of hypoxic exposure on *hif-1α* and *hif-1β* mRNA levels in L3 and adult worms (muscle tissue). The ratios of mRNA levels in hypoxia-exposed worms to those in normoxia-exposed worms are shown (A, *hif-1α* and B, *hif-1β* mRNA levels). Values in adult worms are the means of three experiments ± SD.

4.2. Stage-specific expression of *hif-1α* and *hif-1β* mRNAs

Previous reports on *in vivo* expression patterns and the regulation of *hif-1α* and *hif-1β* mRNAs are controversial. It has been generally considered that both *hif-1* mRNAs are constitutively expressed and that the stability of HIF-1 is regulated primarily at the post-transcriptional level in an oxygen-dependent manner (Powell et al., 2002; Wang et al., 1995). However, conflicting reports have demonstrated that *hif-1α* and/or *hif-1β* mRNA expression are affected by oxygen concentrations in various organisms: rats, birds, and fish (Catron et al., 2001; Rahman and Thomas, 2007; Wiener et al., 1996). In these organisms, particularly in hypoxia-tolerant rats and fish, HIF-1α expression is upregulated at both the transcriptional and post-transcriptional level by hypoxic exposure (Rahman and Thomas, 2007; Shams et al., 2004).

A. suum is a unique model organism for investigating the relationship between *hif-1* expression and the oxygen conditions, since *A. suum* is exposed to normoxia and hypoxia in its natural habitat during its life cycle. To examine *in vivo* expression patterns of *A. suum hif-1α* and *hif-1β*, mRNA levels at different developmental stages were analyzed by real-time PCR. Fertilized eggs showed 6-fold higher *hif-1α* mRNA levels than adult muscle, while *hif-1β* mRNA expression was similar between eggs and adult muscle. This difference in expression patterns of *hif-1α* and *hif-1β* mRNAs could be attributed to their different roles in embryonic development.

In the free-living nematode *C. elegans*, microarray analysis of developmental gene expression have revealed that expression levels of *hif-1* and *aha-1* (*C. elegans hif-1β*) mRNAs are highest during the larval stage, but both show only 2-fold differences at maximum throughout the life cycle (Jiang et al., 2001b). In contrast, in *A. suum*, both *hif-1α* and *hif-1β* mRNA expression significantly changed during the life cycle. They reached maximum levels at the free-living L3 stage and were 6-fold and 8-fold higher than those during the adult stage, respectively. After infection of the host, both *hif-1* mRNAs gradually decreased with development. Significant transcriptional changes of *A. suum hif-1* indicate that there is a regulatory mechanism for its expression. Given that hypoxic exposure had no effects on *hif-1* mRNA levels at any investigated stages, transcriptions of *A. suum hif-1* appear to be regulated in a stage-specific manner rather than in an oxygen-dependent manner. In the hypoxia-tolerant mole rat *Spalax*, *hif-1α* transcription is induced by hypoxia; however, even in normoxia, *Spalax* maintains 2-fold higher *hif-1α* mRNA levels than that in the hypoxia-sensitive rat *Rattus*, enabling effective responses to hypoxia (Shams et al., 2004). These findings imply that certain hypoxia-tolerant organisms accumulate *hif-1* mRNAs even under normoxia. In *A. suum*, high levels of *hif-1* mRNAs in L3 possibly allow quick and sufficient responses to a sudden change of oxygen concentration after ingestion by the host by regulating genes responsible for anaerobic energy metabolism.

4.3. Hypoxia-responsive elements located in 5′-upstream regions of A. suum complex II genes

One of the characteristic features of the HIF-1 pathway is its broad range of target genes. One subset of target genes regulated by HIF-1 encodes various glycolytic enzymes that are robustly upregulated during hypoxia, contributing to metabolic adaptation (Bunn and Poyton, 1996; Seagroves et al., 2001). In addition, recent studies have demonstrated functional crosstalk between the HIF pathway and mitochondria.

In human cells, HIF-1 regulates the replacement of a key subunit of the mitochondrial cytochrome *c* oxidase (COX, also known as complex IV) from COX4-1 to COX4-2 to maximize the efficiency of mitochondrial respiration under hypoxia (Fukuda et al., 2007). Conversely, it has been shown that inhibition of SDH activity (activity of aerobic complex II) results in the accumulation of succinate in the cells, which reduces the enzymatic activity of prolyl hydroxylases by product inhibition. This leads to HIF-1α stabilization and consequently HIF-1 activation (Selak et al., 2005).

Our previous study showed that the expression of the stage-specific isoforms of *A. suum* complex II is regulated at the transcriptional level, enabling metabolic adaptation to hypoxia in the host (Amino et al., 2000, 2003). Considering the importance of structural rearrangements of complex II under hypoxic conditions, a regulatory mechanism between HIF-1 and the expression of complex II subunits is expected to be present. Sequence analysis of 5′-upstream regions of complex II genes identified putative HREs, suggesting that HIF-1 directly regulates the expression of stage-specific complex II isoforms, although the expression of the adult-type Fp appears to be regulated by other factors regardless of hypoxia.

5. Conclusions

In the present study, we cloned *hif-1* cDNAs from *A. suum* and found unique characteristics of their expression patterns. Stage-specific *hif-1* expression may reflect an evolved strategy for hypoxia adaptation, although the regulatory mechanisms are yet to be elucidated. The N-TAD of HIF-1α showed unique sequences distinct from those of other organisms, suggesting that target genes of *A. suum* HIF-1 may be different from known targets. Although further investigation is required to determine the functional role of *A. suum* HIF-1 in the adaptation to hypoxic conditions of adult worms, we consider that it is plausible that HIF-1 is associated with stage-specific metabolic transitions, including the rearrangement of the complex II structure.

Adaptation to changes in the oxygen environment is an important aspect of parasitism, and studies of its regulatory mechanisms will reveal adaptive strategies of parasites in the host.

Supplementary data to this article can be found online at http://dx.doi.org/10.1016/j.gene.2012.12.025.

Acknowledgments

We thank Dr. Takeshi Hatta and Dr. Takeharu Miyoshi for technical support with animal experiments. This study was mainly supported by in part by a Grant-in-aid for Creative Scientific Research (Grant 18GS0314), a Grant-in-aid for Scientific Research on Priority Areas (18073004) from the Japanese Society for the Promotion of Science, the Targeted Proteins Research Program from the Japanese Ministry of Education, Science, Culture, Sports and Technology (MEXT), for research on emerging and re-emerging infectious diseases from the Japanese Ministry of Health and Welfare, and partly by the Programme for Promotion of Basic and Applied Researches for Innovations in Bio-oriented Industry (BRAIN).

References

Amino, H., et al., 2000. Stage-specific isoforms of *Ascaris suum* complex II: the fumarate reductase of the parasitic adult and the succinate dehydrogenase of free-living larvae share a common iron-sulfur subunit. Mol. Biochem. Parasitol. 106, 63–76.

Amino, H., et al., 2003. Isolation and characterization of the stage-specific cytochrome b small subunit (CybS) of *Ascaris suum* complex II from the aerobic respiratory chain of larval mitochondria. Mol. Biochem. Parasitol. 128, 175–186.

Beischlag, T., et al., 2004. Recruitment of thyroid hormone receptor/retinoblastoma-interacting protein 230 by the aryl hydrocarbon receptor nuclear translocator is required for the transcriptional response to both dioxin and hypoxia. J. Biol. Chem. 279, 54620–54628.

Bunn, H., Poyton, R., 1996. Oxygen sensing and molecular adaptation to hypoxia. Physiol. Rev. 76, 839–885.

Catron, T., Mendiola, M., Smith, S., Born, J., Walker, M., 2001. Hypoxia regulates avian cardiac Arnt and HIF-1alpha mRNA expression. Biochem. Biophys. Res. Commun. 282, 602–607.

Chomczynski, P., Sacchi, N., 1987. Single-step method of RNA isolation by acid guanidinium thiocyanate-phenol-chloroform extraction. Anal. Biochem. 162, 156–159.

Epstein, A., et al., 2001. *C. elegans* EGL-9 and mammalian homologs define a family of dioxygenases that regulate HIF by prolyl hydroxylation. Cell 107, 43–54.

Fukuda, R., Zhang, H., Kim, J., Shimoda, L., Dang, C., Semenza, G., 2007. HIF-1 regulates cytochrome oxidase subunits to optimize efficiency of respiration in hypoxic cells. Cell 129, 111–122.

Gu, J., Milligan, J., Huang, L., 2001. Molecular mechanism of hypoxia-inducible factor 1alpha -p300 interaction. A leucine-rich interface regulated by a single cysteine. J. Biol. Chem. 276, 3550–3554.

Hampton-Smith, R., Peet, D., 2009. From polyps to people: a highly familiar response to hypoxia. Ann. N. Y. Acad. Sci. 1177, 19–29.

Hu, C.J., Sataur, A., Wang, L., Chen, H., Simon, M.C., 2007. The N-terminal transactivation domain confers target gene specificity of hypoxia-inducible factors HIF-1alpha and HIF-2alpha. Mol. Biol. Cell 18, 4528–4542.

Huang, J., Zhao, Q., Mooney, S., Lee, F., 2002. Sequence determinants in hypoxia-inducible factor-1alpha for hydroxylation by the prolyl hydroxylases PHD1, PHD2, and PHD3. J. Biol. Chem. 277, 39792–39800.

Islam, M.K., et al., 2006. Effect of piperazine (diethylenediamine) on the moulying proteome express and pyrophosphate activity of *Ascaris suum* lung-stage larvae. Acta Trop. 99, 208–217.

Ivan, M., et al., 2001. HIFalpha targeted for VHL-mediated destruction by proline hydroxylation: implications for O_2 sensing. Science 292, 464–468.

Iwata, F., et al., 2008. Change of subunit composition of mitochondrial complex II (succinate–ubiquinone reductase/quinol–fumarate reductase) in *Ascaris suum* during the migration in the experimental host. Parasitol. Int. 57, 54–61.
Jaakkola, P., et al., 2001. Targeting of HIF-alpha to the von Hippel–Lindau ubiquitylation complex by O_2-regulated prolyl hydroxylation. Science 292, 468–472.
Jain, S., Dolwick, K., Schmidt, J., Bradfield, C., 1994. Potent transactivation domains of the Ah receptor and the Ah receptor nuclear translocator map to their carboxyl termini. J. Biol. Chem. 269, 31518–31524.
Jiang, B., Rue, E., Wang, G., Roe, R., Semenza, G., 1996. Dimerization, DNA binding, and transactivation properties of hypoxia-inducible factor 1. J. Biol. Chem. 271, 17771–17778.
Jiang, B., Zheng, J., Leung, S., Roe, R., Semenza, G., 1997. Transactivation and inhibitory domains of hypoxia-inducible factor 1alpha. Modulation of transcriptional activity by oxygen tension. J. Biol. Chem. 272, 19253–19260.
Jiang, H., Guo, R., Powell-Coffman, J., 2001a. The *Caenorhabditis elegans hif-1* gene encodes a bHLH-PAS protein that is required for adaptation to hypoxia. Proc. Natl. Acad. Sci. U. S. A. 98, 7916–7921.
Jiang, M., Ryu, J., Kiraly, M., Duke, K., Reinke, V., Kim, S., 2001b. Genome-wide analysis of developmental and sex-regulated gene expression profiles in *Caenorhabditis elegans*. Proc. Natl. Acad. Sci. U. S. A. 98, 218–223.
Kaelin, W.J., Ratcliffe, P., 2008. Oxygen sensing by metazoans: the central role of the HIF hydroxylase pathway. Mol. Cell 30, 393–402.
Kallio, P., Pongratz, I., Gradin, K., McGuire, J., Poellinger, L., 1997. Activation of hypoxia-inducible factor 1alpha: posttranscriptional regulation and conformational change by recruitment of the Arnt transcription factor. Proc. Natl. Acad. Sci. U. S. A. 94, 5667–5672.
Kallio, P., et al., 1998. Signal transduction in hypoxic cells: inducible nuclear translocation and recruitment of the CBP/p300 coactivator by the hypoxia-inducible factor-1alpha. EMBO J. 17, 6573–6586.
Kita, K., Takamiya, S., 2002. Electron-transfer complexes in *Ascaris* mitochondria. Adv. Parasitol. 51, 95–131.
Kita, K., Hirawake, H., Takamiya, S., 1997. Cytochromes in the respiratory chain of helminth mitochondria. Int. J. Parasitol. 27, 617–630.
Kita, K., Hirawake, H., Miyadera, H., Amino, H., Takeo, S., 2002. Role of complex II in anaerobic respiration of the parasite mitochondria from *Ascaris suum* and *Plasmodium falciparum*. Biochim. Biophys. Acta 1553, 123–139.
Komuniecki, R., Harris, B.G., 1995. Carbohydrate and energy metabolism in helminths. In: Marr, J., Mueller, M. (Eds.), Biochemistry and Molecular Biology of Parasites. Academic Press, London, pp. 49–66.
Lando, D., Peet, D., Whelan, D., Gorman, J., Whitelaw, M., 2002a. Asparagine hydroxylation of the HIF transactivation domain a hypoxic switch. Science 295, 858–861.
Lando, D., Peet, D., Gorman, J., Whelan, D., Whitelaw, M., Bruick, R., 2002b. FIH-1 is an asparaginyl hydroxylase enzyme that regulates the transcriptional activity of hypoxia-inducible factor. Genes Dev. 16, 1466–1471.
Li, H., Ko, H., Whitlock, J., 1996. Induction of phosphoglycerate kinase 1 gene expression by hypoxia. Roles of Arnt and HIF1alpha. J. Biol. Chem. 271, 21262–21267.
Minning, D.M., et al., 1999. *Ascaris* haemoglobin is a nitric oxide-activated 'deoxygenase'. Nature 401, 497–502.
Nilsen, T., et al., 1989. Characterization and expression of a spliced leader RNA in the parasitic nematode *Ascaris lumbricoides* var. *suum*. Mol. Cell. Biol. 9, 3543–3547.
Powell, J., Elshtein, R., Forest, D., Palladino, M., 2002. Stimulation of hypoxia-inducible factor-1 alpha (HIF-1alpha) protein in the adult rat testis following ischemic injury occurs without an increase in HIF-1alpha messenger RNA expression. Biol. Reprod. 67, 995–1002.
Powell-Coffman, J., Bradfield, C., Wood, W., 1998. *Caenorhabditis elegans* orthologs of the aryl hydrocarbon receptor and its heterodimerization partner the aryl hydrocarbon receptor nuclear translocator. Proc. Natl. Acad. Sci. U. S. A. 95, 2844–2849.
Pugh, C., O'Rourke, J., Nagao, M., Gleadle, J., Ratcliffe, P., 1997. Activation of hypoxia-inducible factor-1; definition of regulatory domains within the alpha subunit. J. Biol. Chem. 272, 11205–11214.
Rahman, M., Thomas, P., 2007. Molecular cloning, characterization and expression of two hypoxia-inducible factor alpha subunits, HIF-1alpha and HIF-2alpha, in a hypoxia-tolerant marine teleost, Atlantic croaker (*Micropogonias undulatus*). Gene 396, 273–282.
Sakai, C., Tomitsuka, E., Esumi, H., Harada, S., Kita, K., 2012. Mitochondrial fumarate reductase as a target of chemotherapy: from parasites to cancer cells. Biochim. Biophys. Acta 1820, 643–651.
Saruta, F., et al., 1995. Stage-specific isoforms of complex II (succinate–ubiquinone oxidoreductase) in mitochondria from the parasitic nematode, Ascaris suum. J. Biol. Chem. 270, 928–932.
Seagroves, T.N., et al., 2001. Transcription factor HIF-1 is a necessary mediator of the Pasteur effect in mammalian cells. Mol. Cell. Biol. 21, 3436–3444.
Selak, M.A., et al., 2005. Succinate links TCA cycle dysfunction to oncogenesis by inhibiting HIF-alpha prolyl hydroxylase. Cancer Cell 7, 77–85.
Semenza, G., 2011. Oxygen sensing, homeostasis, and disease. N. Engl. J. Med. 365, 537–547.
Shams, I., Avivi, A., Nevo, E., 2004. Hypoxic stress tolerance of the blind subterranean mole rat: expression of erythropoietin and hypoxia-inducible factor 1 alpha. Proc. Natl. Acad. Sci. U. S. A. 101, 9698–9703.
Shen, C., Nettleton, D., Jiang, M., Kim, S., Powell-Coffman, J., 2005. Roles of the HIF-1 hypoxia-inducible factor during hypoxia response in *Caenorhabditis elegans*. J. Biol. Chem. 280, 20580–20588.
Shimizu, H., et al., 2012. Crystal structure of mitochondrial quinol-fumarate reductase from the parasitic nematode *Ascaris suum*. J. Biochem. 151, 589–592.
Sonnenfeld, M., Ward, M., Nystrom, G., Mosher, J., Stahl, S., Crews, S., 1997. The *Drosophila* tango gene encodes a bHLH-PAS protein that is orthologous to mammalian Arnt and controls CNS midline and tracheal development. Development 124, 4571–4582.
Takamiya, S., et al., 1993. Developmental changes in the respiratory chain of *Ascaris* mitochondria. Biochim. Biophys. Acta 1141, 65–74.
Tielens, A., Van Hellemond, J., 1998. The electron transport chain in anaerobically functioning eukaryotes. Biochim. Biophys. Acta 1365, 71–78.
Tokishita, S., et al., 2006. Tissue-specific expression of a bHLH-PAS protein homologous to ARNT during the development of crustacean *Daphnia magna*. Gene 376, 231–239.
Wang, G., Semenza, G., 1993. Characterization of hypoxia-inducible factor 1 and regulation of DNA binding activity by hypoxia. J. Biol. Chem. 268, 21513–21518.
Wang, G., Jiang, B., Rue, E., Semenza, G., 1995. Hypoxia-inducible factor 1 is a basic-helix-loop-helix-PAS heterodimer regulated by cellular O_2 tension. Proc. Natl. Acad. Sci. U. S. A. 92, 5510–5514.
Wang, J., et al., 2011. Deep small RNA sequencing from the nematode *Ascaris* reveals conservation, functional diversification, and novel developmental profiles. Genome Res. 21, 1462–1477.
Wiener, C., Booth, G., Semenza, G., 1996. *In vivo* expression of mRNAs encoding hypoxia-inducible factor 1. Biochem. Biophys. Res. Commun. 225, 485–488.
Zelzer, E., Wappner, P., Shilo, B., 1997. The PAS domain confers target gene specificity of *Drosophila* bHLH/PAS proteins. Genes Dev. 11, 2079–2089.